

---

# Adaptive Region-Based Active Learning

---

Corinna Cortes<sup>1</sup> Giulia DeSalvo<sup>1</sup> Claudio Gentile<sup>1</sup> Mehryar Mohri<sup>1,2</sup> Ningshan Zhang<sup>3</sup>

## Abstract

We present a new active learning algorithm that adaptively partitions the input space into a finite number of regions, and subsequently seeks a distinct predictor for each region, both phases actively requesting labels. We prove theoretical guarantees for both the generalization error and the label complexity of our algorithm, and analyze the number of regions defined by the algorithm under some mild assumptions. We also report the results of an extensive suite of experiments on several real-world datasets demonstrating substantial empirical benefits over existing single-region and non-adaptive region-based active learning baselines.

## 1. Introduction

In many learning problems, including document classification, image annotation, and speech recognition, large amounts of unlabeled data are at the learner’s disposal at practically no cost. In contrast, reliable labeled data is often more costly to acquire, since it requires careful assessments by human labelers. To limit that cost, in *active learning*, the learner seeks to request as few labels as possible to learn an accurate predictor. This is an attractive learning scenario with significant practical benefits, which remains a challenging theoretical and algorithmic setting.

The literature on active learning is very broad. Thus, we give only a brief discussion of previous work here and refer the reader to (Dasgupta, 2011) for an in-depth survey of the main algorithmic and theoretical ideas, as well as its current challenges. For separable problems, Cohn et al. (1994) introduced the CAL algorithm, which only requires a logarithmic number of label requests,  $\log(\frac{1}{\epsilon})$ , to obtain  $\epsilon$ -accuracy. Later, other on-line active learning algorithms for general hypothesis classes and distributions were designed with guarantees both for generalization and label complexity in the agnostic setting (Freund et al., 1997; Balcan et al., 2006; Hanneke, 2007; Dasgupta et al., 2008; Beygelzimer

et al., 2009; 2010; Huang et al., 2015; Zhang & Chaudhuri, 2014), and in the separable settings (Dasgupta, 2004; Golovin & Krause, 2017; Nowak, 2011; Tosh & Dasgupta, 2017).

The theoretical analysis of the label complexity of active learning for various hypothesis classes and data distributions has been discussed in several publications (Dasgupta, 2006; Castro & Nowak, 2008; Koltchinskii, 2010; Hanneke & Yang, 2015; Hanneke, 2014; Musmann & Liang, 2018). In particular, for hypothesis sets consisting of linear separators, a series of publications gave margin-based on-line active learning algorithms that admit guarantees under some specific distributional assumptions (Dasgupta et al., 2005; Balcan et al., 2007; Balcan & Long, 2013; Awasthi et al., 2015; Zhang, 2018).

For all these algorithms, the hypothesis set or *version space*  $\mathcal{H}$  is fixed beforehand and, over time, as more labeled information is acquired, it is gradually shrunk to rule out hypotheses too far from the best-in-class hypothesis. This paper initiates the study of an alternative family of algorithms where the hypothesis set  $\mathcal{H}$  is first expanded over time before shrinking. Specifically, we consider active learning algorithms that *adaptively* partition the input space into a finite number of disjoint regions, each equipped with the hypothesis set  $\mathcal{H}$ , and that subsequently seek a distinct predictor for each region. Such algorithms can achieve a substantially better performance, as shown by our theoretical analysis and largely demonstrated by our experiments.

The design of such algorithms raises several questions: How should the input space be partitioned to ensure an improvement in overall performance? How can labels be requested most effectively across regions to learn an accurate predictor per region? Can we provide generalization and label complexity guarantees? In this paper, we tackle these questions and devise an algorithm for this problem, called Adaptive Region-Based Active Learning (ARBAL), benefiting from favorable theoretical guarantees. From a theoretical standpoint, there are several challenging problems: ensuring that the region-specific best-in-class hypothesis is not discarded, the selection of the splitting criteria, and the dependency of the final generalization bound on such criteria.

Of course, if a beneficial partition of the input space is available to the learner, as assumed in the related work of

---

<sup>1</sup>Google Research, New York, NY <sup>2</sup>Courant Institute of Mathematical Sciences, New York, NY <sup>3</sup>New York University, New York, NY. Correspondence to: Ningshan Zhang <nzhang@stern.nyu.edu>.

Cortes et al. (2019b), then no further work is needed to adaptively seek one. In practice, however, such strong oracle information may not be available and, even when a natural pre-partitioning of the input space is available, without recourse to labeled data, it is not guaranteed to help improve the generalization error. Furthermore, we will not assume that dividing the input space is always beneficial. However, if there exists indeed a partition such that a region-specific predictor performs significantly better than a global one, then, with high probability, ARBAL will find it. Otherwise, no split is made and ARBAL works just like a single-region active learning algorithm. In practice, in almost all cases we tested, ARBAL splits the input space into multiple regions and achieves a significant performance improvement.

Another line of work somewhat related to our paper is the hierarchical sampling approach of Dasgupta & Hsu (2008) in the *pool-based setting* of active learning, further analyzed by (Uner et al., 2013) and (Kpotufe et al., 2015), where the learner receives as input a batch of unlabeled points to select from. However, it is important to stress that the methods proposed in those papers rely on (hierarchical) clusterability assumptions of the data that help save labels, while, here, we are more concerned with a problem in model selection for active learning, where splitting the input space is likely to improve generalization rather than reducing label complexity.

In summary, we present an active learning algorithm, ARBAL, that adaptively partitions the input space and performs region-based active learning. Our theoretical results (Theorem 3 and Theorem 9) show that, remarkably, when the algorithm splits the input space into  $K$  regions, modulo a standard term in  $O(1/\sqrt{T})$  decreasing with the number of rounds  $T$ , the generalization error of ARBAL is close to  $R^* - \gamma(K - 1)$ , where  $R^*$  is the best-in-class error for the unpartitioned original input space and  $\gamma > 0$  a parameter of the algorithm. Thus, when at least one split is made by ARBAL ( $K > 1$ ), then, for  $T$  sufficiently large, the error of the algorithm is close to a quantity strictly smaller than the original best-in-class error! Moreover, we show that, under mild theoretical assumptions, ARBAL indeed splits the original input space into multiple subregions (Proposition 4 and Corollary 5). Our experiments confirm that this almost always occurs (Section 5). This significant theoretical improvement over even the original best-in-class error is further corroborated by our extensive experimental study with 25 datasets where, in most cases, ARBAL achieves a better performance than the best active learning algorithm working with the original single region.

The rest of this paper is structured as follows. In Section 2, we introduce the preliminaries relevant to our discussion and give a more formal definition of the learning scenario. In Section 3, we present our new learning algorithm, ARBAL,

and justify its splitting criterion via theoretical guarantees. In Section 4, we provide generalization and label complexity bounds for ARBAL in terms of a key parameter for the splitting criterion, and the number of regions partitioned. Moreover, in Section 4.2 we show that, under some natural assumptions about the data distribution, ARBAL benefits from guaranteed improvement over IWAL (Beygelzimer et al., 2009). In Section 5, we report the results of a series of experiments on multiple datasets, demonstrating the substantial benefits of ARBAL over existing non-region-based active learning algorithms, such as IWAL and margin-based uncertainty sampling, and over the nonadaptive region-based active learning baseline ORIWAL (Cortes et al., 2019b).

## 2. Learning scenario

We now discuss the learning scenario, starting with some preliminary definitions. Let  $\mathcal{X} \subseteq \mathbb{R}^D$  denote the input space,  $\mathcal{Y} = \{-1, +1\}$  the output space, and  $\mathcal{D}$  an unknown distribution over  $\mathcal{X} \times \mathcal{Y}$ . We denote by  $\mathcal{D}_{\mathcal{X}}$  the marginal distribution of  $\mathcal{D}$  over  $\mathcal{X}$  and, given a prediction space  $\mathcal{Z} \subseteq \mathbb{R}$ , we denote by  $\ell: \mathcal{Z} \times \mathcal{Y} \rightarrow [0, 1]$  a loss function, which we assume to be  $\mu$ -Lipschitz with respect to its first argument, for some constant  $\mu > 0$ . Let  $\mathcal{H}$  be a family of hypotheses consisting of functions mapping  $\mathcal{X}$  to  $\mathcal{Z}$ . Then, the generalization error or expected loss of a hypothesis  $h \in \mathcal{H}$  is denoted by  $R(h)$  and defined as  $R(h) = \mathbb{E}_{(x,y) \sim \mathcal{D}}[\ell(h(x), y)]$ .

We consider the on-line setting of active learning where, at each round  $t \in [T] = \{1, \dots, T\}$ , the learner receives as input a point  $x_t \in \mathcal{X}$  drawn i.i.d. according to  $\mathcal{D}_{\mathcal{X}}$  and must decide to request or not its label  $y_t$ . The decision is final and cannot be retroactively changed. At the end of  $T$  rounds, the learner returns a hypothesis  $\hat{h}_T \in \mathcal{H}$ . In this setting, two conflicting quantities determine the performance of an on-line active learning algorithm: its label complexity, that is, the number of labels it has requested over  $T$  rounds, and the generalization error  $R(\hat{h}_T)$  of the hypothesis it returns.

In the standard case where the hypothesis set  $\mathcal{H}$  is given beforehand, the learner seeks a single best predictor from  $\mathcal{H}$ . Here, we consider instead the setup where the algorithm adaptively partitions the input space  $\mathcal{X}$  into  $K$  regions  $\mathcal{X}_1, \dots, \mathcal{X}_K$ , each equipped with a copy of the hypothesis set  $\mathcal{H}$  and with  $K$  upper-bounded by some parameter  $\kappa \geq 1$ . Given the partition  $\mathcal{X}_1, \dots, \mathcal{X}_K$ , the hypothesis  $\hat{h}_T$  returned by the algorithm after  $T$  rounds admits the following form:  $\hat{h}_T(x) = \sum_{k=1}^K 1_{x \in \mathcal{X}_k} \hat{h}_{k,T}(x)$ , where  $\hat{h}_{k,T}$  is the hypothesis chosen after  $T$  rounds by the algorithm for region  $\mathcal{X}_k$ .

Let  $\mathbf{p}_k = \mathbb{P}(\mathcal{X}_k)$  denote the probability of region  $\mathcal{X}_k$  with respect to  $\mathcal{D}_{\mathcal{X}}$ ,  $k \in [K]$ , and let  $R_k(h)$  denote the conditional expected loss of a hypothesis  $h$  on region  $\mathcal{X}_k$ , that is  $R_k(h) = \mathbb{E}_{(x,y) \sim \mathcal{D}}[\ell(h(x), y) | x \in \mathcal{X}_k]$ . By definition, we have  $R(h) = \sum_{k=1}^K \mathbf{p}_k R_k(h)$  for any hypothesis  $h$ . We

assume the learner has access to large amounts of *unlabeled* data, which can be used to accurately estimate  $p_k$ . In fact, our results can be easily adapted to the case where the  $p_k$ s are estimated via a collection of unlabeled examples requested on-the-fly. While this would not add much to our analysis in terms of technical difficulty, it would make the entire theoretical effort unnecessarily more cluttered.

We denote by  $h^* \in \mathcal{H}$  the overall best-in-class hypothesis over  $\mathcal{X}$  (single region before any splitting) and by  $h_k^* \in \mathcal{H}$  the  $k$ -th region's best-in-class hypothesis, that is,  $h^* = \operatorname{argmin}_{h \in \mathcal{H}} R(h)$  and  $h_k^* = \operatorname{argmin}_{h \in \mathcal{H}} R_k(h)$ . We will also use as shorthand the following notation:  $R^* = R(h^*)$  and  $R_k^* = R_k(h_k^*)$ .

Observe that minimizing the generalization error within each region  $\mathcal{X}_k$  individually is equivalent to minimizing the overall error over the larger set  $\mathcal{H}_{[K]} = \{ \sum_{k=1}^K 1_{x \in \mathcal{X}_k} h_k(x) : h_k \in \mathcal{H} \}$ . Clearly, the performance of the best predictor in  $\mathcal{H}_{[K]}$  is always at least as favorable as that of the best predictor in  $\mathcal{H}$ , but it can be considerably better, especially when the algorithm chooses a large  $K$ , or when the local performances of  $h_k^*$ s with large  $p_k$  are substantially superior to that of  $h^*$  on the same regions.

### 3. Algorithm

Our algorithm, called ARBAL (Adaptive Region-Based Active Learning), is an on-line active learning algorithm that *adaptively* partitions the input space into subregions. ARBAL adopts a label requesting policy similar to that of the single-region IWAL algorithm of [Beygelzimer et al. \(2009\)](#), which is based on the largest possible disagreement among the current set of hypotheses on the current input: at round  $t$ , given the hypothesis set  $\mathcal{H}_t$  and input point  $x_t \in \mathcal{X}$ , IWAL flips a coin  $Q_t \in \{0, 1\}$  with bias  $p_t = p(x_t)$  defined by

$$p_t = \max_{h, h' \in \mathcal{H}_t, y \in \mathcal{Y}} \ell(h(x_t), y) - \ell(h'(x_t), y).$$

If  $Q_t = 1$ , then the label of  $x_t$  is requested and the algorithm receives  $y_t$ , otherwise no label is revealed. Since the loss function  $\ell$  takes values in  $[0, 1]$ , the requesting probability  $p_t \in [0, 1]$  is well defined. IWAL then seeks to shrink the current set  $\mathcal{H}_t$  to reduce the querying probability  $p_t$  for future inputs, while, at the same time, keeping (with high probability) the overall best-in-class hypothesis in this set. At the end of  $T$  rounds, IWAL returns the importance-weighted empirical risk minimizer  $\hat{h}_T = \operatorname{argmin}_{h \in \mathcal{H}_T} \sum_{t=1}^T Q_t \ell(h(x_t), y_t) / p_t$ .

Our techniques and ideas for splitting are illustrated with IWAL, since IWAL works with any hypothesis set and bounded loss function, and admits generalization guarantees with no distributional assumption. In contrast, CAL ([Cohn et al., 1994](#)) assumes a separable case; DHM ([Dasgupta et al., 2008](#)) and  $A^2$  ([Balcan et al., 2006](#)) are designed

for the 0-1 loss, and many other margin-based algorithms only work for linear classifiers. Furthermore, for the separable case ( $R^* = 0$ ), the recent work of ([Cortes et al., 2019b](#)) proposes an enhanced version of IWAL, called EI-WAL, whose label complexity is in the order of  $\log \left( \frac{|\mathcal{H}|}{\epsilon} \right)$ , thereby matching the bound of CAL and DHM. That being said, our techniques can be easily applied to other algorithms available in the literature, so long as they have valid concentration bounds, such as Corollary 1 of the DHM paper ([Dasgupta et al., 2008](#)), and Theorem 1 of [Cortes et al. \(2019b\)](#). In that case, we just need to change the splitting criterion accordingly, and our theoretical analysis can then be easily adapted to the new concentration bound.

Our algorithm can be viewed as an adaptive region-based version of IWAL, where the label requesting policy just described and the shrinking procedure are applied at the regional level. As already mentioned, the following questions arise when designing the algorithm: (1) How should we determine the regions? (2) Can we learn to adaptively partition the input space into favorable subregions, using actively requested labels? We now explicitly address both questions and describe our algorithm in detail.

The pseudocode of ARBAL is given in [Algorithm 1](#). The algorithm admits two phases: in the first phase (*split phase*), the algorithm partitions the input space into  $K$  disjoint regions while actively requesting labels according to IWAL's policy on the regional level. This phase is constrained by two input parameters:  $\kappa$  limits the maximum number of regions generated ( $K \leq \kappa$ ), and  $\tau$  caps the maximal number of online rounds for this phase. [Section 3.1](#) describes in detail the main subroutine of this phase, SPLIT ([Algorithm 2](#)), including the splitting conditions that guarantee a significant improvement in generalization ability resulting from the split. Whenever the algorithm decides to split, each resulting region is equipped with a copy of the original hypothesis set  $\mathcal{H}$ . Notice that the algorithm actively selects labels in this phase, even if it does not shrink the hypothesis set(s), and thus it still requests fewer labels than passive learning. For simplicity, the regions will be axis-aligned rectangles, though more convoluted splitting shapes are clearly possible (see [Section 5](#)).

In the second phase (*IWAL phase*), ARBAL runs IWAL separately on each of the regions produced by the first phase, to learn a good predictor per region. After  $T$  rounds, ARBAL returns  $\hat{h}_T$ , which combines region-specific importance-weighted empirical risk minimizers  $\hat{h}_{k,T}$ . In [Section 3.2](#), we describe the IWAL phase, and discuss its connections to ORI-WAL ([Cortes et al., 2019b](#)).

One question naturally arises: Why do we separate the learning horizon into two phases, where we first determine the partition, and then perform region-based learn-

**Algorithm 1** ARBAL( $\mathcal{H}, \tau, \kappa, (\gamma_t)_{t \in [T]}$ )

---

```

 $K \leftarrow 1, \mathcal{X}_1 \leftarrow \mathcal{X}, \mathcal{H}_1 \leftarrow \mathcal{H}$ 
for  $t \in [T]$  do
    Observe  $x_t$ ; set  $k_t \leftarrow k$  such that  $x_t \in \mathcal{X}_k$ 
     $p_t \leftarrow \max_{h, h' \in \mathcal{H}_{k_t}, y \in \mathcal{Y}} \ell(h(x_t), y) - \ell(h'(x_t), y)$ 
     $Q_t \leftarrow \text{BERNOULLI}(p_t)$ 
    if  $Q_t = 1$  then
         $y_t \leftarrow \text{LABEL}(x_t)$ 
    end if
    if  $t \leq \tau$  and  $K < \kappa$  then
         $\mathcal{X}_l, \mathcal{X}_r \leftarrow \text{SPLIT}(\mathcal{X}_{k_t}, \gamma_t)$            # split phase
        if split then
             $K \leftarrow K + 1, \mathcal{X}_{k_t} \leftarrow \mathcal{X}_l, \mathcal{X}_K \leftarrow \mathcal{X}_r$ 
             $\mathcal{H}_K \leftarrow \mathcal{H}, \mathcal{H}_{k_t} \leftarrow \mathcal{H}$ 
        end if
    else
         $\mathcal{H}_{k_t} \leftarrow \text{UPDATE}(\mathcal{H}_{k_t})$            # IWAL phase
    end if
end for
return  $\hat{h}_T \leftarrow \sum_{k=1}^K 1_{x \in \mathcal{X}_k} \hat{h}_{k,T}$ 

```

---

**Algorithm 2** SPLIT( $\mathcal{X}_k, \gamma$ )

---

```

for  $d \in [D]$  and  $c \in \mathbb{R}$  do
     $(\mathcal{X}_l, \mathcal{X}_r) \leftarrow \text{REGSPLIT}(\mathcal{X}_k, d, c)$ 
     $\gamma_{d,c} \leftarrow \text{pk} \left[ L_{k,t}(\hat{h}_{k,t}) - L_{k,t}(\hat{h}_{lr,t}) - \sqrt{\frac{2\sigma_T}{T_{k,t}}} \right]$ 
end for
 $(d^*, c^*) \leftarrow \text{argmax}_{d \in [D], c \in \mathbb{R}} \gamma_{d,c}$ 
if  $\gamma_{d^*, c^*} \geq \gamma$  then
     $\mathcal{X}_l^* \leftarrow \{x \in \mathcal{X}_k : x[d^*] \leq c^*\}$            # split
     $\mathcal{X}_r^* \leftarrow \{x \in \mathcal{X}_k : x[d^*] > c^*\}$ 
    return  $\mathcal{X}_l^*, \mathcal{X}_r^*$ 
else
    return  $\emptyset$            # no split
end if

```

---

ing? Given all possible partitions of the input space, why not running IWAL with the family of hypotheses containing all possible partitions of  $\mathcal{X}$  with leaf predictors  $h_k \in \mathcal{H}$ , that is,  $\mathbb{H} = \{ \sum_{k=1}^{\kappa} 1_{x \in \mathcal{X}_k} h_k : h_k \in \mathcal{H}, \cup_{k=1}^{\kappa} \mathcal{X}_k = \mathcal{X}, \mathcal{X}_k \cap \mathcal{X}_{k'} = \emptyset \text{ for } k \neq k' \}$ ? First,  $\mathbb{H}$  is an exceedingly complex hypothesis set, whose complexity can lead to vacuous learning guarantees. Second, its computational cost makes it prohibitive to use with IWAL. Moreover, even if we fix the partition and only vary the predictors in the leaf nodes, as proven in Appendix B, running IWAL with  $\mathbb{H}$  may cost up to  $\kappa$  times more labels than running IWAL separately within each partitioned region. For all these reasons, we adopt the two-phases learning framework.

### 3.1. SPLIT phase

The advantage of region-based learning hinges on the improvement in the best-in-class error after each split, which motivates our splitting subroutine: SPLIT splits a region if and only if the best-in-class error is likely to improve by a strictly positive amount. We will show in Corollary 2 that,

with high-probability, the best-in-class error is guaranteed to decrease from each split.

The pseudocode of SPLIT is given in Algorithm 2. At time  $t$ , SPLIT searches for the most favorable choice of the splitting parameters  $(d, c)$  as follows. Adopting the axis-aligned splitting method commonly used for (binary) decision trees: for a fixed pair  $(d, c)$ , the algorithm calls subroutine REGSPLIT( $\mathcal{X}_k, d, c$ ) to split  $\mathcal{X}_k$  into a left region  $\mathcal{X}_l$  ( $x_d \leq c$ ) and a right region  $\mathcal{X}_r$  ( $x_d > c$ ), and then computes a *confidence gap*  $\gamma_{d,c}$  as defined in Algorithm 2, where  $L_{k,t}(h)$  denotes the importance-weighted empirical risk of hypothesis  $h$  on region  $\mathcal{X}_k$ ,

$$L_{k,t}(h) = \frac{1}{T_{k,t}} \sum_{s \in [t], x_s \in \mathcal{X}_k} \frac{Q_s}{p_s} \ell(h(x_s), y_s),$$

where  $T_{k,t} = |\{s \in [t] : x_s \in \mathcal{X}_k\}|$  is the number of samples that have been observed in region  $\mathcal{X}_k$  up to time  $t$ , and  $\sigma_T = \kappa D \log \left[ \frac{8T^3 |\mathcal{H}|^3 \kappa D}{\delta} \right]$  denotes the slack term. Furthermore,  $\hat{h}_{k,t} = \text{argmin}_{h \in \mathcal{H}} L_{k,t}(h)$  denotes the empirical risk minimizer (ERM) on  $\mathcal{X}_{k_t}$ . Similarly,  $\hat{h}_{l,t}$  and  $\hat{h}_{r,t}$  denote the ERM of region  $\mathcal{X}_l$  and  $\mathcal{X}_r$ , respectively, and  $\hat{h}_{lr,t} = 1_{x \in \mathcal{X}_l} \hat{h}_{l,t} + 1_{x \in \mathcal{X}_r} \hat{h}_{r,t}$  is the combination of the two region-specific ERMs. The confidence gap  $\gamma_{d,c}$  serves as a conservative estimate of the improvement in the best-in-class error. SPLIT searches for the maximum confidence gap over all distinct pairs:  $(d^*, c^*) = \text{argmax}_{d,c} \gamma_{d,c}$ . When  $\gamma_{d^*, c^*}$  is larger than the pre-specified threshold parameter  $\gamma$ , it splits with  $(d^*, c^*)$  and allocates to the two newly created regions the same initial hypothesis set  $\mathcal{H}$  (see Algorithm 1), otherwise it does not split.

To implement the SPLIT subroutine, we maintain an array of region labels of past samples, and  $D$  sorted arrays of past samples according to each of the  $D$  coordinates. At time  $t$ , for each coordinate  $d \in [D]$ , it takes  $O(\log(t))$  to insert  $x_t$  into the sorted array, and  $O(t)$  to compute the key term  $L_{k,t}$  for all  $t+1$  splitting thresholds on the sorted array. Here, we use the fact that although there are infinitely many possible splitting threshold values, we only need to consider  $t+1$  many thresholds to distinguish the  $t$  feature values  $\{x_{s,d} : s \in [t]\}$ . It also takes  $O(t)$  to update the region labels of past samples after split, and thus a total of  $O(tD)$  to run SPLIT at time  $t$ . Furthermore, as already mentioned in Section 2, we assume access to a set  $U$  of unlabeled samples to estimate all the  $p_k$ s. To do so, we maintain a binary tree corresponding to the splits. A new split converts a leaf node  $u_i$  with number of elements  $|u_i| \leq |U|$  into an internal node at the cost of  $O(|u_i|)$ . The cost of updating the tree for the  $\kappa$  splits in order to estimate all  $p_k$ s is hence  $O(\sum_{i=1}^{\kappa} |u_i|)$ , where the sum is over all the internal nodes of the tree.

Alternatively, these probabilities can be estimated incrementally during the on-line execution of the algorithm, and our

theoretical analysis can be extended along these lines using a union bound similar to the one in Lemma 1’s proof.

We now introduce some additional notation before discussing the theoretical guarantees of the SPLIT algorithm. Let  $h_k^*$ ,  $h_l^*$ ,  $h_r^*$  be the best-in-class predictors on region  $\mathcal{X}_k$ ,  $\mathcal{X}_l$ , and  $\mathcal{X}_r$ , respectively, and denote by  $h_{l_r}^* = 1_{x \in \mathcal{X}_l} h_l^* + 1_{x \in \mathcal{X}_r} h_r^*$ . Then, the improvement in the best-in-class error after this split is  $\mathfrak{p}_k[R_k(h_k^*) - R_k(h_{l_r}^*)]$ . The following concentration lemma relates the improvement in the best-in-class error to its empirical counterparts, which leads to the theoretical guarantee for the SPLIT subroutine (Corollary 2). Its proof uses a martingale concentration bound, as well as covering number techniques to guarantee that the high-probability bound holds uniformly for any possible sequence of splitting. The proof is given in Appendix C.

**Lemma 1.** *With probability at least  $1 - \delta/4$ , for all binary trees with (at most)  $\kappa$  leaf nodes, the improvement in the minimal empirical error by splitting concentrates around the improvement in the best-in-class error:*

$$\left| [R_k(h_k^*) - R_k(h_{l_r}^*)] - [L_{k,t}(\hat{h}_{k,t}) - L_{k,t}(\hat{h}_{l_r,t})] \right| \leq \sqrt{\frac{2\sigma_T}{T_{k,t}}}.$$

**Corollary 2.** *With probability at least  $1 - \delta/4$ , for all splits made by ARBAL, the improvement in the best-in-class error is at least  $\gamma_t$ , where  $\gamma_t$  is the threshold at the time of split.*

Corollary 2 guarantees that, with high-probability, whenever ARBAL splits, the best-in-class error is strictly improved by at least  $\gamma_t > 0$ . This yields the fundamental advantage of region-based learning.

One challenge ARBAL faces is that, whenever it chooses to split, it commits to competing against a more accurate predictor, that is the region-specific best-in-class hypothesis on the refined regions. To ensure success, we need to guarantee not only that the best-in-class over the current region or those over subregions after the split are not pruned out, but also that the best-in-class hypothesis over any *future* region produced after further splitting remains in the hypothesis space that will be given as input to ARBAL’s second phase.

One can show that, if ARBAL prunes out some hypotheses before the split phase has ended, it may lose the future best-in-class predictor, and thus fail dramatically. As a simple example, consider the binary classification problem depicted in Figure 1, where the unlabeled data is uniformly distributed within a square, and the true classification boundary admits a zig-zag shape (the left plot of Figure 1). If the learner uses the class of linear separators as the initial hypothesis set  $\mathcal{H}$ , then, after receiving a certain number of labeled samples, it finds that the best performing hypothesis is approximately the diagonal separator from bottom left to top right. Suppose the algorithm would now trim  $\mathcal{H}$  to only maintain separators performing similarly to the diagonal

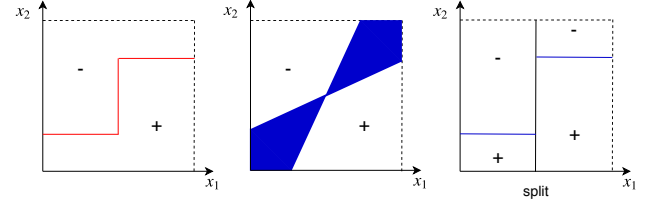


Figure 1: The input space  $\mathcal{X}$  is a (2-dimensional) square. Left: the true classification boundary (in red) as a function of  $x_1$  and  $x_2$ . Middle: (approximately) the current hypothesis space (shaded blue area) after trimming an initial set of linear separators given several labeled samples. Right: the best-in-class predictors (in blue) when the input space  $\mathcal{X}$  splits into two regions  $\mathcal{X}_l$  and  $\mathcal{X}_r$  from the middle of  $x_1$ .

separator, with decision surfaces indicated by the shaded area in the middle plot of Figure 1. If later on, the learner splits the input space (the square) into two regions (left and right rectangles in the right plot of Figure 1), then the best-in-class separators for the two rectangles are horizontal separators. Clearly, the two horizontal best-in-class separators are not contained in the current  $\mathcal{H}$  (which is meant to apply to the entire input space). In summary, trimming  $\mathcal{H}$  before making splits introduces the risk of losing the best-in-class separators on the partitioned regions. This is the reason why ARBAL maintains throughout the split phase the original hypothesis space  $\mathcal{H}$ . The shrinkage of  $\mathcal{H}$  only takes place during the IWAL phase, presented next.

### 3.2. IWAL phase

In this phase, with the regions  $\mathcal{X}_1, \dots, \mathcal{X}_K$  being fixed, ARBAL runs a separate IWAL subroutine on each one of them, requesting labels and reducing the hypothesis space from  $\mathcal{H}$  to region-specific  $\mathcal{H}_k, \forall k \in [K]$ . As the algorithm requests labels,  $\mathcal{H}_k$  shrinks towards the best-in-class hypothesis on region  $\mathcal{X}_k$ . The hypothesis space is updated according to the IWAL update rule, which is derived from the concentration bound. Specifically, we update the hypothesis space  $\mathcal{H}_{k,t}$  sitting on region  $\mathcal{X}_k$  at time  $t$  by

$$\mathcal{H}_{k,t} = \left\{ h \in \mathcal{H}_{k,t-1} : L_{k,t}(h) \leq \min_{h \in \mathcal{H}_{k,t-1}} L_{k,t}(h) + \sqrt{\frac{8\sigma_T}{T_{k,t}}} \right\}.$$

Thus, in this phase, ARBAL freezes the regions  $\mathcal{X}_1, \dots, \mathcal{X}_K$ , allowing no further splits, and requests labels and shrinks the set of hypotheses hosted by each such region.

Starting with a fixed partition makes the second phase of ARBAL very similar to the learning scenario recently investigated by Cortes et al. (2019b), who proposed the ORIWAL algorithm for this learning scenario. In particular, during the second phase, we could also run the ORIWAL algorithm to achieve additional improvement in generalization error. Since ORIWAL is orthogonal to the main contribution of this

paper, we do not discuss it at length here.

## 4. Theoretical analysis

In this section, we present generalization error and label complexity guarantees for the ARBAL algorithm. We first need some definitions and concepts from [Beygelzimer et al. \(2009\)](#). Define the distance  $\rho(f, g)$  between two hypotheses  $f, g \in \mathcal{H}$  as  $\rho(f, g) = \mathbb{E}_{(x,y) \sim \mathcal{D}} |\ell(f(x), y) - \ell(g(x), y)|$ .<sup>1</sup> The generalized disagreement coefficient  $\theta(\mathcal{D}, \mathcal{H})$  of a class of functions  $\mathcal{H}$  with respect to distribution  $\mathcal{D}$  is defined as the minimum value of  $\theta$ , such that for all  $r > 0$ ,

$$\mathbb{E}_{x \sim \mathcal{D}_x} \left[ \sup_{h \in \mathcal{H}, \rho(h, h^*) \leq r, y \in \mathcal{Y}} |\ell(h(x), y) - \ell(h^*(x), y)| \right] \leq \theta r.$$

Since ARBAL calls IWAL as a subroutine, the theoretical results of ARBAL directly depend on those of IWAL, which are summarized in Theorem 6 in Appendix A.

Recall the definition of the confidence gap  $\gamma$  in Algorithm 2, which is the minimum value of the confidence gap  $\gamma_{d,c}$  that allows ARBAL to split a region. We discuss ARBAL under two settings: using a fixed threshold  $\gamma$ , and using a time-varying and data-dependent adaptive threshold  $\gamma_t$ .

### 4.1. ARBAL with a fixed $\gamma$

Suppose we run ARBAL with a fixed threshold  $\gamma$ . The label complexity of the algorithm depends on the region-based disagreement coefficient  $\theta_k = \theta(\mathcal{D}_k, \mathcal{H})$ , where  $\mathcal{D}_k = \mathcal{D}|_{\mathcal{X}_k}$  is defined as the conditional distribution of  $x$  on region  $\mathcal{X}_k$ . Let  $\theta_{\max} = \max_{k \in K} \theta_k$  denote the maximum disagreement coefficient across regions, and let  $r_0 = \max_{h \in \mathcal{H}} \rho(h, h^*)$ . Let  $\mathcal{F}_t$  denotes the  $\sigma$ -algebra generated by  $(x_1, y_1, Q_1), \dots, (x_t, y_t, Q_t)$ .

**Theorem 3.** *Assume that a run of ARBAL over  $T$  rounds has split the input space into  $K$  regions. Then, for any  $\delta > 0$ , with probability at least  $1 - \delta$ , the following inequality holds:*

$$R(\hat{h}_T) \leq R_U + \sqrt{\frac{32K\sigma_T}{T}} + \frac{16K\sigma_T}{T},$$

where  $R_U = R^* - \gamma(K - 1)$  is an upper bound on the best-in-class error obtained by ARBAL. Moreover, with probability at least  $1 - \delta$ , the expected number of labels requested,  $\tau_T = \sum_{t=1}^T \mathbb{E}_{x_t \sim \mathcal{D}_x} [p_t | \mathcal{F}_{t-1}]$ , satisfies

$$\tau_T \leq \min\{2\theta r_0, 1\}\tau + 4\theta_{\max}(T - \tau) \left[ R_U + 8\sqrt{\frac{K\sigma_T}{T - \tau}} \right] + \sqrt{32K\sigma_T}.$$

<sup>1</sup>This definition of  $\rho(f, g)$  slightly differs from the original definition in [Beygelzimer et al. \(2009\)](#), and it improves the label complexity bound of IWAL by a constant. See Appendix A for more details.

The proof is given in Appendix C. It combines the learning guarantee of IWAL (Theorem 6) with those for splitting (Corollary 2). Theorem 3 shows that, with high probability, the generalization error of the hypothesis returned by ARBAL is close to  $R_U = R^* - \gamma(K - 1)$ , which is a more favorable benchmark than the single-region best-in class error  $R^*$  by  $\gamma(K - 1)$ . We will show later that, under natural assumptions, with high probability, there is at least one split, which implies  $\gamma(K - 1) > 0$  (Proposition 4). Furthermore, the reduction in the best-in-class error also improves label complexity: when  $T \gg \tau$ , the label complexity of ARBAL is  $O(R_U T)$  compared to IWAL's  $O(R^* T)$ .

In practice, we set  $\gamma = \Omega(\sqrt{\sigma_T/T})$  to ensure that the generalization bound in Theorem 3 is more favorable than the generalization bound of IWAL (Theorem 6). We give more details on how to set this fixed  $\gamma$  in Appendix C (see comments following the proof of Theorem 3).

There is a critical trade-off when determining the key parameters  $\tau$  and  $\kappa$ . With a larger  $\tau$  and  $\kappa$ , ARBAL is likely to split into more regions and thus admits a smaller  $R_U$ . On the other hand, a larger  $\tau$  means a longer split phase, where ARBAL requests labels more often compared to the original IWAL algorithm since ARBAL does not shrink the hypothesis set  $\mathcal{H}$  during this phase, and a larger  $\kappa$  yields a larger  $\sigma_T$ , which slightly affects the generalization error. Nevertheless, our experimental results show that larger values of  $\tau$  and  $\kappa$  almost always improve the final excess risk, at the expense of higher computational cost.

### 4.2. ARBAL with adaptive $\gamma_t$

The learning guarantees of Theorem 3 depend on the number of regions  $K$  defined by the algorithm. Given any fixed value of  $\gamma$ , however, there is no guarantee on the number of times ARBAL splits within the first  $\tau$  rounds (the duration of the first phase). In the worst case when  $K = 1$ , ARBAL offers no improvement over IWAL, yet ARBAL requests more labels than IWAL during the initial  $\tau$  rounds.

In this section, we show that by adopting a time-varying and data-dependent splitting threshold  $\gamma_t$ , we can enable SPLIT to split more often, and thus achieve an enhanced performance guarantee. To do so, we make additional assumptions on the potential gain of splitting.

Let  $\mathcal{X}_k$  be an intermediate region created during the split phase, possibly the original input space  $\mathcal{X}$ . Assume that for any such  $\mathcal{X}_k$ , there exists at least one way of splitting  $\mathcal{X}_k$  into  $\mathcal{X}_l \cup \mathcal{X}_r$  such that the conditional improvement in the best-in-class error is at least  $\rho$ :  $R_k(h_k^*) - R_k(h_{lr}^*) \geq \rho$ , where  $\rho > 0$  is a positive constant. With this assumption, we can derive upper bounds on the time ARBAL splits when run with a time-varying adaptive  $\gamma_t = \mathbb{P}(\mathcal{X}_{k_t})\rho/2$ .

**Proposition 4.** *Let ARBAL be run with  $\gamma_t = \rho \mathbb{P}(\mathcal{X}_{k_t})/2$ .*

Then, for any  $\delta > 0$ , with probability at least  $1 - \delta/2$ , the first split occurs before round  $\lceil 2\sigma_T(\frac{4}{\rho} + 1)^2 \rceil$ .

Thus, when  $\tau \geq \lceil 2\sigma_T(\frac{4}{\rho} + 1)^2 \rceil$ , with high probability, ARBAL will split  $\mathcal{X}$  and reduce the best-in-class error by at least  $\rho/2$ , according to Proposition 4 and Corollary 2. In Appendix C, we prove a more general version (Lemma 11) that upper bounds the time of split for all regions created during the split phase.

If we further assume that the splitting with at least  $\rho$  improvement in the best-in-class error results in regions that are not too small, i.e.,  $\min\{\mathbb{P}(\mathcal{X}_l), \mathbb{P}(\mathcal{X}_r)\} \geq c\mathbb{P}(\mathcal{X}_k)$ , with  $0 < c < 0.5$ , then we can also prove a lower bound on the number of splits.

**Corollary 5.** *Let ARBAL run with  $\gamma_t = \mathbb{P}(\mathcal{X}_{k_t})\rho/2$ . Then, with probability at least  $1 - \delta/2$ , ARBAL splits more than  $\min\left\{\log_{1/c}\left[\frac{\tau}{2\sigma_T(\frac{4}{\rho}+1)^2}\right], \kappa - 1\right\}$  times by the end of the split phase.*

Corollary 5 gives the minimal number of splits under the assumptions made in this section. It states that, as the duration of the split phase  $\tau$  increases, or as the conditional improvement  $\rho$  increases, or as the minimal proportion of subregion size  $c$  increases, ARBAL tends to make more splits and therefore achieves a better generalization guarantee. Note that the lower bound in Corollary 5 tends to be loose, as it assumes that ARBAL keeps splitting the smallest region, which is unlikely to be the case in practice. In Appendix C, we combine Proposition 4 and Corollary 5 to give an upper bound on the final best-in-class error after the splits by ARBAL.

Note that the true value of  $\rho$  is the property of the underlying distribution, and to accurately estimate  $\rho$  is an open question that is beyond the scope of this paper. One practical solution is to explore  $\rho$  on various orders of magnitude, e.g. (0.1, 0.01) etc., such that ARBAL makes a reasonable number of splits. We set  $\rho = 0.01$  in our experiments.

## 5. Experiments

In this section, we report the results of a series of experiments. We tested 24 binary classification datasets from the UCI and openml repositories, and also the MNIST dataset with 3 and 5 as the two classes, which is standard binary classification task extracted from the MNIST dataset (e.g., (Crammer et al., 2009)). Table 1 in Appendix D lists summary statistics for these datasets. For ease of experimental comparison, for datasets with large input dimension  $D$ , we followed the preprocessing step in (Cortes et al., 2019b), retaining only the first 10 principal components of the original feature vectors. Due to space limitations, in this section we show the results on several medium-sized datasets. The results for the remaining datasets are pro-

vided in Appendix D. For each experiment, we randomly shuffled the dataset, ran the algorithms on the first half of the data (so that the number of active learning rounds  $T$  equals  $N/2$ ), and tested the classifier returned on the remaining half to measure misclassification loss. We only showed results on the first  $10^{3.5} \approx 3000$  requested labels, which are enough to differentiate the performances among various algorithms. We repeated this process 50 times on each dataset, and report average results with standard error across the 50 repetitions. We use the logistic loss function  $\ell$  defined for all  $(x, y) \in \mathcal{X} \times \mathcal{Y}$  and hypotheses  $h: \mathcal{X} \rightarrow \mathbb{R}$  by  $\ell(h(x), y) = \log(1 + e^{-yh(x)})$ , which we then rescale to  $[0, 1]$ . The initial hypothesis set  $\mathcal{H}$  consists of 3,000 randomly drawn hyperplanes with bounded norms. As mentioned in Section 4.1, larger values of  $\tau$  and  $\kappa$  almost always yield better final excess risk. Thus, we chose  $\kappa = 20$  and allow the first phase to run at most  $\tau = 800$  rounds so as to make ARBAL fully split into the desired number of regions on almost all datasets. Since the slack term  $\sigma_T$  derived from high-probability analyses are typically overly conservative, we simply use  $0.01/\sqrt{T_k}$  in the SPLIT subroutine.

**ARBAL with fixed or adaptive  $\gamma$ .** We first compare ARBAL with fixed  $\gamma$  to ARBAL with an adaptive  $\gamma_t$ . Figure 2 plots the misclassification loss versus the number of labels requested on four datasets. The vertical lines indicate the label counts when ARBAL transitions from the first to the second phase, and the legends give the average number of resulting regions  $K$  the algorithms produce. Adaptive  $\gamma_t$  tends to split into more regions and to exit the split phase earlier, and hence often results in superior prediction performance over fixed  $\gamma$ . Thus, in the rest of this section, we show the performance with adaptive  $\gamma_t$ . Results on other datasets (see Appendix D) show similar patterns. During the active learning split phase, even though ARBAL does not shrink the hypothesis set(s), both versions are observed to request labels in only 50% - 90% of the rounds, which is far less than passive learning.

**ARBAL vs. ORIWAL.** Since the key idea of ARBAL is the informed adaptive splitting criterion, we compare ARBAL with the ORIWAL algorithm of Cortes et al. (2019b), a “non-adaptive splitting” algorithm that first randomly generates  $\kappa$  regions, and then runs region-based active learning on these regions. The regions of ORIWAL are obtained from terminal nodes of random binary trees, that is, binary trees with random splitting coordinates and thresholds (hence, they are axis-aligned rectangles, as for ARBAL). Figure 3 shows that ARBAL quickly takes over (recall that the  $x$  axis is on log scale) and performs substantially better than ORIWAL, on eight datasets covered by Figure 3. Results on other datasets show similar patterns, even though ORIWAL sometimes uses more regions than ARBAL, since ARBAL may not always fully split into  $\kappa$  regions. These results empirically verify the advantage of an adaptive splitting criterion.

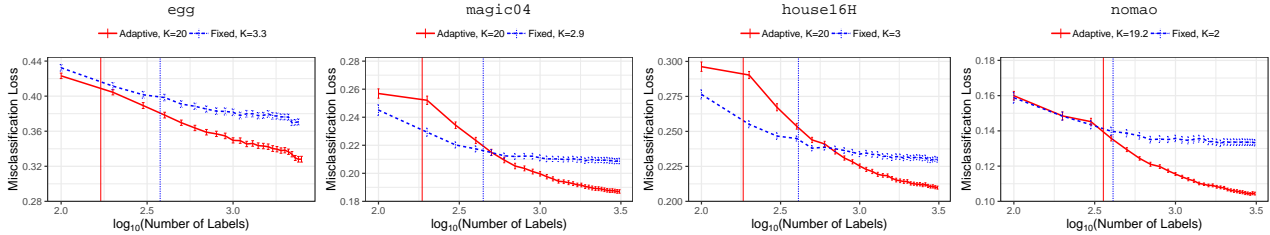


Figure 2: Misclassification loss of ARBAL with fixed and adaptive threshold  $\gamma$  on held out test data vs. number of labels requested ( $\log_{10}$  scale), with  $\kappa = 20$  and  $\tau = 800$ . The vertical lines indicate the end of the first (split) phase.

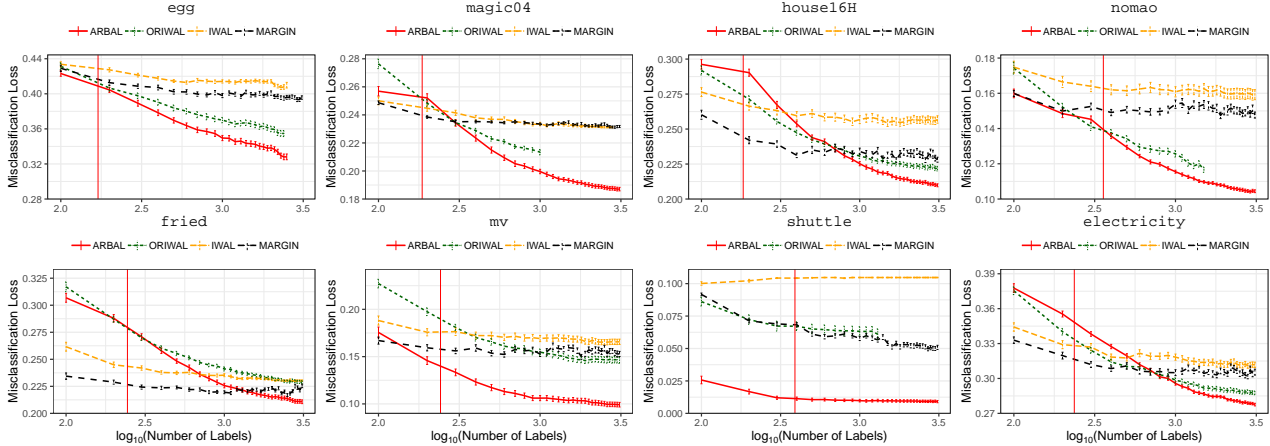


Figure 3: Misclassification loss of ARBAL (with adaptive  $\gamma_t$ ), ORIWAL, IWAL, and MARGIN on hold out test data vs. number of labels requested ( $\log_{10}$  scale), with  $\kappa = 20$  and  $\tau = 800$ . The ARBAL curves are repetitions from Figure 2.

**ARBAL vs. non-splitting baselines.** We also compare ARBAL with the single-region IWAL algorithm, and the single-region MARGIN algorithm, which is a standard uncertainty sampling algorithm that requests the label closest to the decision boundary of the current empirical risk minimizer (note that MARGIN runs under a pool-based setting and thus sees more information than on-line algorithms). Figure 3 shows that MARGIN is a strong baseline that outperforms IWAL on almost all the datasets, sometimes even ORIWAL (e.g. *house16H*), but ARBAL is still more favorable than MARGIN. The difference of errors observed in these plots after consuming much of the sample is essentially due to the difference of the split-region and single-region best-in-class errors, that is,  $R_U$  vs.  $R^*$ , which further corroborates our theory. The results for most other datasets show similar patterns. In fact, ARBAL can also be used with the MARGIN algorithm as a subroutine, which is likely to lead to even better performance but, as with the MARGIN algorithm, that extension would not benefit from any general theoretical guarantee and might actually underperform in some instances where the MARGIN technique can fail.

Finally, as mentioned in Section 3.1, ARBAL is agnostic to the shape of subregions, thus any hierarchical partitioning method could be used in the splitting phase. For instance, we can split a region via an arbitrary separating hyperplane

or via hierarchical clustering, that is, determine two new centers and assign points to the closest center. In Appendix D, we compare axis-aligned binary tree splitting method with hierarchical clustering splitting, using adaptive  $\gamma_t$ . Our results suggest that, for most datasets, splitting via binary trees is more favorable than via hierarchical clustering.

## 6. Conclusion

We presented a novel algorithm for adaptive region-based active learning, and proved that it benefits from favorable generalization and label complexity guarantees. We also studied the extent to which splitting the input space is likely to lead to improved prediction performance. We complemented our theoretical findings by reporting the results of several experiments with our algorithm on standard benchmarks. Our extensive experiments demonstrate substantial performance improvements over existing active learning algorithms such as IWAL and margin-based uncertainty sampling, as well as other region-based baselines that do not rely on adaptively splitting of the input space. Our techniques have been showcased through IWAL-like algorithms (Beygelzimer et al., 2009; Cortes et al., 2019b), but they can be straightforwardly combined with other base active learning algorithms, such as the DHM algorithm from (Dasgupta et al., 2008), achieving similar generalization and



label complexity guarantees.

Altogether, our theory, algorithms, and empirical results provide a new promising solution to active learning, with very important practical benefits. These results also suggest further investigation of the general idea of adaptively refining and enriching the hypothesis set for active learning.

## References

- Awasthi, P., Balcan, M.-F., Haghtalab, N., and Urner, R. Efficient learning of linear separators under bounded noise. In *Proceedings of COLT*, pp. 167–190, 2015.
- Balcan, M.-F. and Long, P. Active and passive learning of linear separators under log-concave distributions. In *Proceedings of COLT*, pp. 288–316, 2013.
- Balcan, M.-F., Beygelzimer, A., and Langford, J. Agnostic active learning. In *Proceedings of ICML*, 2006.
- Balcan, M.-F., Broder, A., and Zhang, T. Margin based active learning. In *International Conference on Computational Learning Theory*, pp. 35–50. Springer, 2007.
- Beygelzimer, A., Dasgupta, S., and Langford, J. Importance weighted active learning. In *Proceedings of ICML*, pp. 49–56. ACM, 2009.
- Beygelzimer, A., Hsu, D. J., Langford, J., and Zhang, T. Agnostic active learning without constraints. In *Proceedings of NIPS*, pp. 199–207, 2010.
- Castro, R. M. and Nowak, R. D. Minimax bounds for active learning. *IEEE Transactions on Information Theory*, 54(5):2339–2353, 2008.
- Chuang, G., DeSalvo, G., Karydas, L., Kagy, J., Ros-tamizadeh, A., and Theeraphol, A. Active learning empirical study. In *NeurIPS2019 LIRE Workshop*, 2019.
- Cohn, D., Atlas, L., and Ladner, R. Improving generalization with active learning. *Machine learning*, 15(2): 201–221, 1994.
- Cortes, C., DeSalvo, G., Gentile, C., Mohri, M., and Zhang, N. Active learning with disagreement graphs. In *Proceedings of ICML*, 2019a.
- Cortes, C., DeSalvo, G., Gentile, C., Mohri, M., and Zhang, N. Region-based active learning. In *Proceedings of AISTATS 2019*, 2019b.
- Cramer, K., Kulesza, A., and Dredze, M. Adaptive regularization of weight vectors. In *Nips*, 2009.
- Dasgupta, S. Analysis of a greedy active learning strategy. In *Advances in neural information processing systems*, pp. 337–344, 2004.
- Dasgupta, S. Coarse sample complexity bounds for active learning. In *Proceedings of NIPS*, pp. 235–242, 2006.
- Dasgupta, S. Two faces of active learning. *Theor. Comput. Sci.*, 412(19):1767–1781, 2011.
- Dasgupta, S. and Hsu, D. Hierarchical sampling for active learning. In *Proceedings of ICML*, pp. 208–215. ACM, 2008.
- Dasgupta, S., Kalai, A. T., and Monteleoni, C. Analysis of perceptron-based active learning. In *International Conference on Computational Learning Theory*, pp. 249–263. Springer, 2005.
- Dasgupta, S., Hsu, D. J., and Monteleoni, C. A general agnostic active learning algorithm. In *Proceedings of NIPS*, pp. 353–360, 2008.
- Freund, Y., Seung, H. S., Shamir, E., and Tishby, N. Selective sampling using the query by committee algorithm. *Machine learning*, 28(2-3):133–168, 1997.
- Golovin, D. and Krause, A. Adaptive submodularity: A new approach to active learning and stochastic optimization. In *arXiv:1003.3967*, 2017.
- Hanneke, S. A bound on the label complexity of agnostic active learning. In *Proceedings of ICML*, pp. 353–360. ACM, 2007.
- Hanneke, S. Theory of disagreement-based active learning. *Foundations and Trends in Machine Learning*, 7(2-3): 131–309, 2014.
- Hanneke, S. and Yang, L. Minimax analysis of active learning. *The Journal of Machine Learning Research*, 16(1): 3487–3602, 2015.
- Huang, T.-K., Agarwal, A., Hsu, D., Langford, J., and E. Schapire, R. Efficient and parsimonious agnostic active learning. In *Proceedings of NIPS*, 2015.
- Koltchinskii, V. Rademacher complexities and bounding the excess risk in active learning. *Journal of Machine Learning Research*, 11(Sep):2457–2485, 2010.
- Kpotufe, S., Urner, R., and Ben-David, S. Hierarchical label queries with data-dependent partitions. In *Proceedings of COLT*, pp. 1176–1189, 2015.
- Mussmann, S. and Liang, P. On the relationship between data efficiency and error for uncertainty sampling. In *PMLR 80: Proceedings of the 35th International Conference on Machine Learning*, pp. 3674–3682, 2018.
- Nowak, R. The geometry of generalized binary search. *IEEE Transactions on Information Theory*, 57(12):7893–7906, 2011.

- Tosh, C. and Dasgupta, S. Diameter-based active learning. In *Thirty-fourth International Conference on Machine Learning (ICML)*, 2017.
- Uerner, R., Wulff, S., and Ben-David, S. PLAL: Cluster-based active learning. In *Proceedings of COLT*, pp. 376–397, 2013.
- Zhang, C. Efficient active learning of sparse halfspaces. In *Proceedings of COLT*, 2018.
- Zhang, C. and Chaudhuri, K. Beyond disagreement-based agnostic active learning. In *Proceedings of NIPS*, pp. 442–450, 2014.

## A. Guarantees for IWAL

The disagreement coefficient  $\theta$  is a complexity measure widely used in disagreement-based active learning problems. In particular, [Hanneke \(2007\)](#) proved upper bounds for the label complexity for the  $A^2$  algorithm in terms of  $\theta$ . [Dasgupta et al. \(2008\)](#) also gave an upper bound for their DHM algorithm using  $\theta$ . The reader is referred to [Hanneke \(2014\)](#) for a more extensive analysis of the disagreement coefficient as related to active learning.

In [Beygelzimer et al. \(2009\)](#), the distance  $\rho$  is defined as

$$\rho(f, g) = \mathbb{E}_{x \sim \mathcal{D}_x} \sup_{y \in \mathcal{Y}} |\ell(f(x), y) - \ell(g(x), y)|,$$

while the distance  $\rho$  in Section 4 is defined in a slightly different manner as

$$\rho(f, g) = \mathbb{E}_{(x, y) \sim \mathcal{D}} |\ell(f(x), y) - \ell(g(x), y)|. \quad (1)$$

[\(Cortes et al., 2019a\)](#) showed that the new definition of  $\rho$  in Eq. (1) removes a constant  $K_\ell$  from the label complexity bound of IWAL, where  $K_\ell$  depends on the loss function and is always greater than 1. Thus this new definition of  $\rho$  improves the label complexity bound of IWAL.

**Theorem 6** ([\(Beygelzimer et al., 2009\)](#)). *Let  $\hat{h}_T$  be the hypothesis output by IWAL after  $T$  rounds. For all  $\delta > 0$ , with probability at least  $1 - \delta$ , for any  $t \in [T]$ ,*

$$R(\hat{h}_T) \leq R^* + 2\sqrt{\frac{8 \log \left[ \frac{2T(T+1)|\mathcal{H}|^2}{\delta} \right]}{T}}, \quad (2)$$

$$\mathbb{E}_{x_t \sim \mathcal{D}_x} [p_t | \mathcal{F}_{t-1}] \leq 4\theta \left[ R^* + \sqrt{\frac{8 \log \left[ \frac{2(t-1)t|\mathcal{H}|^2}{\delta} \right]}{t-1}} \right], \quad (3)$$

where  $\mathcal{F}_t$  denotes the  $\sigma$ -algebra generated by  $(x_1, y_1, Q_1), \dots, (x_t, y_t, Q_t)$ .

Thus, the generalization error of the returned hypothesis  $\hat{h}_T$  is close to that of the best-in-class, while the expected number of labels requested after  $T$  rounds is in  $O(R^*T)$ .

## B. Region-Based Active Learning

The following results are adapted from [\(Cortes et al., 2019b\)](#). Lemma 7 relates the region-specific disagreement coefficients  $\theta_k = \theta(\mathcal{D}_k, \mathcal{H})$  to the overall disagreement coefficient  $\theta(\mathcal{D}, \mathcal{H}_{[\kappa]})$ , where  $\mathcal{H}_{[\kappa]} = \{ \sum_{k=1}^{\kappa} 1_{x \in X_k} h_k(x) : h_k \in \mathcal{H} \}$ . Theorem 8 compares the learning guarantees of running with  $\mathcal{H}_{[\kappa]}$  and running IWAL within each region separately.

**Lemma 7.** *The generalized disagreement coefficient  $\theta(\mathcal{D}, \mathcal{H}_{[\kappa]})$  satisfies  $\theta(\mathcal{D}, \mathcal{H}_{[\kappa]}) \leq \sum_{k=1}^{\kappa} \theta(\mathcal{D}_k, \mathcal{H})$ .*

*Proof.* Denote  $h^* = \operatorname{argmin}_{h \in \mathcal{H}_{[\kappa]}} R(h)$ , and  $h_k^* = \operatorname{argmin}_{h \in \mathcal{H}} R_k(h)$ . Recall that  $\mathcal{D}_k = \mathcal{D}|_{X_k}$  denotes the conditional distribution of  $x$  on  $X_k$ , and that  $h^*$  is defined as  $h^* = \sum_{k=1}^{\kappa} 1_{x \in X_k} h_k^*$ . Extending the definitions in Section 4, we define

$$\rho_k(f, g) = \mathbb{E}_{(x, y) \sim \mathcal{D}_k} |\ell(f(x), y) - \ell(g(x), y)|.$$

Given the hypothesis set  $\mathcal{H}$  and any real  $r > 0$ , define

$$B_k(f, r) = \{g \in \mathcal{H} : \rho_k(f, g) \leq r\}.$$

For a set of non-negative values  $\lambda = \{\lambda_1, \dots, \lambda_\kappa\}$ , let

$$G_\lambda(h^*, r) = \left\{ \sum_{k=1}^{\kappa} 1_{x \in X_k} g_k : g_k \in B_k(h_k^*, \lambda_k r) \right\}.$$

We first show that, for any  $\lambda$  satisfying  $\sum_{k=1}^{\kappa} p_k \lambda_k \leq 1$ ,  $G_\lambda(h^*, r) \subseteq B(h^*, r)$ . Let  $g = \sum_{k=1}^{\kappa} 1_{x \in X_k} g_k$ , where  $g_k \in B_k(h_k^*, \lambda_k r)$ . Then,

$$\begin{aligned} \rho(h^*, g) &= \mathbb{E}_{(x, y) \sim \mathcal{D}} |\ell(h^*(x), y) - \ell(g(x), y)| \\ &= \sum_{k=1}^{\kappa} p_k \mathbb{E}_{(x, y) \sim \mathcal{D}_k} |\ell(h_k^*(x), y) - \ell(g_k(x), y)| \\ &\leq \sum_{k=1}^{\kappa} p_k \lambda_k r \leq r. \end{aligned}$$

Thus,  $\{ \cup_{\lambda: \sum_{k=1}^{\kappa} p_k \lambda_k \leq 1} G_\lambda(h^*, r) \} \subseteq B(h^*, r)$ . On the other hand, if there exists a hypothesis  $h$  such that

$$h \in B(h^*, r) \setminus \left\{ \cup_{\lambda: \sum_{k=1}^{\kappa} p_k \lambda_k \leq 1} G_\lambda(h^*, r) \right\},$$

let this  $h$  be of the form  $h = \sum_{k=1}^{\kappa} 1_{x \in X_k} h_k$ . Then,

$$\rho(h^*, h) = \sum_{k=1}^{\kappa} p_k \rho_k(h_k^*, h_k) \leq r \Rightarrow \sum_{k=1}^{\kappa} p_k \frac{\rho_k(h_k^*, h_k)}{r} \leq 1.$$

Obviously,  $h_k \in B_k(h_k^*, \rho_k(h_k^*, h_k))$ . Thus, let  $\lambda = \left\{ \frac{\rho_1(h_1^*, h_1)}{r}, \dots, \frac{\rho_\kappa(h_\kappa^*, h_\kappa)}{r} \right\}$ , then  $\sum_{k=1}^{\kappa} p_k \lambda_k \leq 1$ , and  $h \in G_\lambda(h^*, r)$  by definition. We have a contradiction. Therefore,

$$\left\{ \cup_{\lambda: \sum_{k=1}^{\kappa} p_k \lambda_k \leq 1} G_\lambda(h^*, r) \right\} = B(h^*, r).$$

Given the equivalence above, for any  $k \in [\kappa]$ ,

$$\begin{aligned} \mathcal{H} \cap B(h^*, r) &= \mathcal{H} \cap \left\{ \cup_{\lambda: \sum_{k=1}^{\kappa} p_k \lambda_k \leq 1} G_\lambda(h^*, r) \right\} \\ &= \mathcal{H} \cap \left\{ \cup_{\lambda_k \leq 1/p_k} B_k(h_k^*, \lambda_k r) \right\} \quad (4) \end{aligned}$$

$$= B_k(h_k^*, r/p_k). \quad (5)$$

Equation (4) follows from the definition of  $G_\lambda(h^*, r)$ . Putting everything together, we have for any  $r \geq 0$ ,

$$\begin{aligned} & \mathbb{E}_{x \sim \mathcal{D}} \sup_{h \in B(h^*, r)} \sup_y |\ell(h(x), y) - \ell(h^*(x), y)| \\ &= \sum_{k=1}^{\kappa} \mathbf{p}_k \mathbb{E}_{x \sim \mathcal{D}_k} \sup_{h \in B(h^*, r)} \sup_y |\ell(h(x), y) - \ell(h^*(x), y)| \\ &= \sum_{k=1}^{\kappa} \mathbf{p}_k \mathbb{E}_{x \sim \mathcal{D}_k} \sup_{y, h_k \in B(h_k^*, \frac{r}{\mathbf{p}_k})} |\ell(h_k(x), y) - \ell(h_k^*(x), y)| \end{aligned} \quad (6)$$

$$\begin{aligned} & \leq \sum_{k=1}^{\kappa} \mathbf{p}_k \theta(\mathcal{D}_k, \mathcal{H}) r / \mathbf{p}_k \quad (7) \\ &= \left( \sum_{k=1}^{\kappa} \theta(\mathcal{D}_k, \mathcal{H}) \right) r. \end{aligned}$$

Equation (6) holds due to the equivalence in (5), and inequality (7) follows from the definition of  $\theta(\mathcal{D}_k, \mathcal{H})$ .

Finally, recall the definition of  $\theta(\mathcal{D}, \mathcal{H}_{[\kappa]})$ :

$$\begin{aligned} \theta(\mathcal{D}, \mathcal{H}_{[\kappa]}) &= \inf \left\{ \forall r \geq 0, \right. \\ & \left. \mathbb{E}_{x \sim \mathcal{D}} \sup_{h \in B(h^*, r)} \sup_y |\ell(h(x), y) - \ell(h^*(x), y)| \leq \theta r \right\}. \end{aligned}$$

Therefore  $\theta(\mathcal{D}, \mathcal{H}_{[\kappa]}) \leq \sum_{k=1}^{\kappa} \theta(\mathcal{D}_k, \mathcal{H}_k)$ , which concludes the proof.  $\square$

Combining Lemma 7 with the learning guarantee of IWAL (Theorem 6), we obtain the following result.

**Theorem 8.** *Assume  $\theta_k = \theta(\mathcal{D}_k, \mathcal{H})$  is the same across all regions  $\mathcal{X}_k, k \in [\kappa]$ . Consider running with IWAL with  $\mathcal{H}_{[\kappa]}$  (Method 1) and running IWAL with  $\mathcal{H}$  on each region separately (Method 2). Then, the hypothesis returned by both methods admit comparable generalization error guarantees, but on average running with  $\mathcal{H}_{[\kappa]}$  would request up to  $\kappa$  times more labels.*

*Proof.* Denote  $h^* = \operatorname{argmin}_{h \in \mathcal{H}_{[\kappa]}} R(h)$ . Let  $N = |\mathcal{H}|$ , and  $\theta_0 = \theta(\mathcal{D}_k, \mathcal{H})$ , for all  $k \in [\kappa]$ , so that  $|\mathcal{H}_{[\kappa]}| = N^\kappa$  and, from Lemma 7,  $\theta(\mathcal{D}, \mathcal{H}_{[\kappa]}) \leq \kappa \theta_0$ . According to the learning guarantee of IWAL, with probability at least  $1 - \delta$ , Method 1 (running with  $\mathcal{H}_{[\kappa]}$ ) satisfies

$$R(h_T^{(1)}) \leq R(h^*) + O\left(\sqrt{\frac{\log(TN^{2\kappa}/\delta)}{T}}\right), \quad (8)$$

$$\tau_T^{(1)} \leq 4\kappa\theta_0 \left[ R(h^*)T + O\left(\sqrt{T \log(TN^{2\kappa}/\delta)}\right) \right]. \quad (9)$$

In addition, with probability at least  $1 - \delta$ , Method 2 (running

IWAL within each region separately) satisfies

$$R(h_T^{(2)}) \leq R(h^*) + \sum_{k=1}^{\kappa} \mathbf{p}_k O\left(\sqrt{\frac{\log(T|N|^{2\kappa}/\delta)}{T_k}}\right), \quad (10)$$

$$\begin{aligned} \tau_T^{(2)} &\leq \sum_{k=1}^{\kappa} 4\theta_0 \left[ R_k(h^*)T\mathbf{p}_k + O(\sqrt{2T\mathbf{p}_k \log(2TN^{2\kappa}/\delta)}) \right] \\ &= 4\theta_0 \left[ R(h^*)T + \sum_{k=1}^{\kappa} O(\sqrt{2T\mathbf{p}_k \log(2TN^{2\kappa}/\delta)}) \right]. \end{aligned} \quad (11)$$

Replacing  $T_k$  with  $T\mathbf{p}_k + O(\sqrt{T})$  in the RHS of (10), and using the fact that  $\sum_{k=1}^{\kappa} \sqrt{\mathbf{p}_k} \leq \sqrt{\kappa}$ , we obtain

$$R(h_T^{(2)}) \leq R(h^*) + O\left(\sqrt{\frac{\kappa \log(T|N|^{2\kappa}/\delta)}{T}}\right). \quad (12)$$

Comparing the upper bound on the generalization error of Method 2 (Eq. (12)) to that of Method 1 (Eq. (8)), we conclude that the two algorithms admit comparable learning guarantees.

On the other hand, comparing the proportion of labels requested per round, we have

$$\begin{aligned} \tau_T^{(1)}/T &\leq 4\kappa\theta_0 R(h^*) + O\left(\frac{1}{\sqrt{T}}\right), \\ \tau_T^{(2)}/T &\leq 4\theta_0 R(h^*) + O\left(\frac{1}{\sqrt{T}}\right). \end{aligned}$$

Thus, Method 1 may request up to  $\kappa$  times more labels than Method 2.  $\square$

## C. Proofs

For simplicity of presentation, all results are stated and proven under the assumption that the loss function  $\ell$  is  $\mu$ -Lipschitz with  $\mu \leq 1$ . This is the case, e.g., for hinge loss and logistic loss.

**Lemma 1.** *With probability at least  $1 - \delta/4$ , for all binary trees with (at most)  $\kappa$  leaf nodes, the improvement in the minimal empirical error by splitting concentrates around the improvement in the best-in-class error:*

$$\begin{aligned} & \left| [R_k(h_k^*) - R_k(h_{lr}^*)] - [L_{k,t}(\hat{h}_{k,t}) - L_{k,t}(\hat{h}_{lr,t})] \right| \\ & \leq \sqrt{\frac{2\sigma_T}{T_{k,t}}}. \end{aligned}$$

*Proof.* We first assume that the splitting threshold  $c$  only takes values in pre-specified sets. To be more concrete, when splitting along coordinate  $d$ , the threshold only takes one of the  $C$  pre-specified values:  $c \in \Theta^d = \{\theta_1^d, \dots, \theta_C^d\}$ , where  $\theta_1^d, \dots, \theta_C^d \in \mathbb{R}$  discretize the  $d$ -th coordinate. Given

this assumption, we can upper bound the number of possible binary trees with at most  $\kappa$  regions. Note that for there to be  $\kappa$  regions, there must be  $\kappa - 1$  splits. Also note that, at each split, there are at most  $C \times D$  possible splitting tuples of  $(d, c)$ , where  $D$  is the number of features and  $C$  is the number of possible thresholds. At the  $k$ -th split,  $k \leq \kappa - 1$ , one first chooses which leaf node to split on (there are  $k$  of them), and then picks a splitting tuple, thus there are  $kCD$  possible splitting outcomes. By the multiplication rule in probability, there are a total of

$$(CD) \times (2CD) \times (3CD) \cdots \times ((\kappa - 1)CD) \leq (\kappa CD)^\kappa$$

possible binary trees with  $\kappa$  regions.

We prove this Lemma as follows. We first fix a binary tree and prove concentration inequalities that hold for every internal node of that tree. Next, we take a union bound over the  $(\kappa CD)^\kappa$  trees to extend these inequalities to hold every node of every tree with the given splitting thresholds. Finally, we extend that to trees with arbitrary thresholds using a standard covering number argument.

Fix a binary tree as well as an intermediate region  $k$  during the split phase. Furthermore, fix a  $T_k > 0$  and condition on the event  $T_{k,t} = T_k$ . Then we can drop the time subscript  $t$  from notation, since the tail probability will be determined by  $T_k$  only. To avoid clutter in the notation, we re-index the sample points  $x_1, \dots, x_T$  in such a way that the first  $T_k$  of them fall in region  $\mathcal{X}_k$ .

Define the composite hypothesis set  $\mathcal{H}^2 = \{1_{x \in \mathcal{X}_1} h_1 + 1_{x \in \mathcal{X}_r} h_2 : h_1, h_2 \in \mathcal{H}\}$ ; then  $|\mathcal{H}^2| = |\mathcal{H}|^2$ . Moreover,

$$h_{lr}^* = \operatorname{argmin}_{h \in \mathcal{H}^2} R_k(h), \quad \widehat{h}_{lr} = \operatorname{argmin}_{h \in \mathcal{H}^2} L_k(h).$$

Fix a pair of hypotheses  $f \in \mathcal{H}$ ,  $g \in \mathcal{H}^2$ . For brevity, define  $\ell(h, h'; x, y) = \ell(h(x), y) - \ell(h'(x), y)$ , and then the random variable

$$Z_t = \frac{Q_t}{p_t} \ell(f, g; x_t, y_t).$$

Then,  $\{Z_t, t \in [T_k]\}$  are i.i.d. random variables, since when the hypothesis set  $\mathcal{H}$  is fixed we have  $p_t = p(x_t)$ , being  $p(x)$  the average disagreement of  $\mathcal{H}$  on  $x$ . Thus  $p_t$  only depends on  $x_t$  and  $\mathcal{H}$ , and is independent of the past (unlike the standard IWAL).

By definition,  $|Z_t| \leq 1$  since at point  $x_t$ ,

$$\max_{f \in \mathcal{H}, g \in \mathcal{H}^2} \ell(f, g; x_t, y_t) = \max_{f \in \mathcal{H}, g \in \mathcal{H}} \ell(f, g; x_t, y_t) \leq p_t,$$

where recall the label request probability

$$p_t = \max_{h, h' \in \mathcal{H}, y_t \in \mathcal{Y}} \ell(h, h'; x_t, y_t).$$

Furthermore,

$$\mathbb{E}_{\substack{Q_t \sim p_t \\ (x_t, y_t) \sim \mathcal{D} | \mathcal{X}_k}} [Z_t] = R_k(f) - R_k(g).$$

Applying Hoeffding's inequality to  $Z_t$  yields

$$\begin{aligned} \mathbb{P} \left( \left| \sum_{t=1}^{T_k} Z_t - \mathbb{E}[Z_t] \right| \geq T_k \Delta_{T_k} \right) &\leq 2e^{-\frac{T_k \Delta_{T_k}^2}{2}} \\ &= \frac{\delta}{4T_k(T_k + 1)|\mathcal{H}|^3}, \end{aligned}$$

where  $\Delta_{T_k} = \sqrt{\frac{2 \log(8|\mathcal{H}|^3 T_k(T_k + 1)/\delta)}{T_k}}$ . A union bound over all possible values of  $T_k$  and all pairs of  $(f, g) \in \mathcal{H} \times \mathcal{H}^2$  allows us to conclude that, with probability at least  $1 - \delta/4$ , for all  $T_k$  and all  $(f, g)$ ,

$$|R_k(f) - R_k(g) - L_k(f) + L_k(g)| \leq \Delta_{T_k}. \quad (13)$$

Thus,

$$\begin{aligned} R_k(h_k^*) - R_k(h_{lr}^*) &\geq R_k(h_k^*) - R_k(\widehat{h}_{lr}) \\ &\geq L_k(h_k^*) - L_k(\widehat{h}_{lr}) - \Delta_{T_k} \\ &\geq L_k(\widehat{h}_k) - L_k(\widehat{h}_{lr}) - \Delta_{T_k}, \end{aligned}$$

where the first inequality follows from the definition of  $h_{lr}^*$ , the second inequality follows from (13) (since  $h_k^* \in \mathcal{H}$  and  $\widehat{h}_{lr} \in \mathcal{H}^2$ ), and the last inequality follows from the definition of  $\widehat{h}_k$ .

Similarly,

$$\begin{aligned} R_k(h_k^*) - R_k(h_{lr}^*) &\leq R_k(\widehat{h}_k) - R_k(h_{lr}^*) \\ &\leq L_k(\widehat{h}_k) - L_k(h_{lr}^*) + \Delta_{T_k} \\ &\leq L_k(\widehat{h}_k) - L_k(\widehat{h}_{lr}) + \Delta_{T_k}. \end{aligned}$$

To take a union bound over at most  $\kappa$  regions, as well as over the  $(\kappa CD)^\kappa$  possible binary trees, we replace  $\delta$  with  $\frac{\delta}{\kappa(\kappa CD)^\kappa}$  in the expression of  $\Delta_{T_k}$ . Thus, we have the concentration results of Eq. (13) hold uniformly over all  $\kappa$  leaf nodes and over all binary trees constructed from the pre-specified thresholds, with  $\Delta_{T_k} = \sqrt{\frac{2\kappa \log(8|\mathcal{H}|^3 T_{k,t}(T_{k,t} + 1)\kappa CD/\delta)}{T_{k,t}}}$ .

Finally, by a standard argument, with the  $\mu$ -Lipschitzness of the loss, with  $\mu \leq 1$ , the family of losses of trees with any threshold can be covered by the losses of those with thresholds in  $\Theta$ , where  $\Theta$  is defined by values separated by  $\epsilon$  for each dimension, which has cardinality  $(1/\epsilon)^D$ . Further replacing  $\delta$  with  $\delta\epsilon^D$ , and setting  $\epsilon = 1/T$ , we have  $\Delta_{T_k} = \sqrt{\frac{2\kappa D \log(8|\mathcal{H}|^3 T_{k,t}(T_{k,t} + 1)\kappa TD/\delta)}{T_{k,t}}}$ . Upper bounding  $T_{k,t}(T_{k,t} + 1)$  with  $T^2$  yields Lemma 1.  $\square$

**Corollary 2.** *With probability at least  $1 - \delta/4$ , for all splits made by ARBAL, the improvement in the best-in-class error is at least  $\gamma_t$ , where  $\gamma_t$  is the threshold at the time of split.*

*Proof.* Let ARBAL split at time  $t$  region  $\mathcal{X}_k$  with threshold  $\gamma_t$ . From Lemma 1, with probability at least  $1 - \delta/4$ , for any split that ARBAL makes,

$$\begin{aligned} & \mathbb{P}_k(R_k(h_k^*) - R_k(h_{l_r}^*)) \\ & \geq \mathbb{P}_k\left(L_{k,t}(\hat{h}_{k,t}) - L_k(\hat{h}_{l_r,t}) - \eta_{k,t}\right) \geq \gamma_t, \end{aligned}$$

where the last inequality follows from the definition of  $\gamma_t$  and the splitting criterion.  $\square$

We now proceed to proving Theorem 3, but first we show a version of Theorem 3 with random quantities in it.

**Theorem 9.** *Assume ARBAL runs with a fixed  $\gamma$  and has split the input space into  $K$  regions. Then, with probability at least  $1 - \delta/2$ ,*

$$R(\hat{h}_T) \leq \sum_{k=1}^K \mathbb{P}_k \left[ R_k^* + 4\sqrt{\frac{2\sigma_T}{T_k}} \right] \quad (14)$$

$$\leq R^* - \gamma(K-1) + \sum_{k=1}^K 4\mathbb{P}_k \sqrt{\frac{2\sigma_T}{T_k}}, \quad (15)$$

where  $T_k$  is the total number of unlabeled samples in region  $k$  up to round  $T$ . Moreover, with probability at least  $1 - \delta/2$ ,

$$\begin{aligned} & \sum_{t=1}^T \mathbb{E}_{x \sim \mathcal{D}_x} [p_t | \mathcal{F}_{t-1}] \leq \min\{2\theta r_0, 1\} \tau \\ & + \sum_{k=1}^K 4\theta_k \left[ R_k^* T_k' + 4\sqrt{2T_k' \sigma_T} \right], \end{aligned} \quad (16)$$

where  $T_k'$  is the total number of unlabeled samples in region  $k$  from round  $\tau + 1$  to  $T$ .

*Proof.* By Eq (2) in Theorem 6, for a fixed binary tree and for a fixed region  $k$  resulting from the binary tree, with probability at least  $1 - \delta/4$ , for all  $T_k > 0$ ,

$$R(\hat{h}_{k,T}) - R(h_k^*) \leq 2\sqrt{\frac{8 \log(8T_k(T_k + 1)|\mathcal{H}|^2/\delta)}{T_k}}.$$

Using the same technique as in the proof of Lemma 1, we take a union bound over the (at most)  $\kappa$  regions as well as over the  $(\kappa CD)^\kappa$  possible binary trees and use the Lipschitzness argument, we obtain the first inequality (14) with probability at least  $1 - \delta/4$ . To simplify the notation, we have upper bounded the term in the log,  $T_k(T_k + 1)|\mathcal{H}|^2 \leq T^2|\mathcal{H}|^3$ , to match that in  $\sigma_T$ .

The second inequality (15) follows from Corollary 2, that each split gives at least  $\gamma$  improvement in the error of best-in-class predictors. It follows that with probability at least  $1 - \delta/4$ ,

$$\sum_{k=1}^K \mathbb{P}_k R_k^* \leq R^* - \gamma(K-1).$$

A union bound over (14) and (15) gives the first statement of Theorem 9.

The statement about label complexity (16) follows from the analysis of IWAL's label complexity. Recall that in IWAL, with probability at least  $1 - \delta$ ,

$$\mathbb{E}_{x \sim \mathcal{D}_x} [p_t | \mathcal{F}_{t-1}] \leq 4\theta \left( R^* + \sqrt{\frac{8 \log(2T^2|\mathcal{H}|^2/\delta)}{t-1}} \right),$$

where we upper bound  $(t-1)t$  by  $T^2$  since  $t \in [T]$ . Within the split phase, the space of hypotheses remains  $\mathcal{H}$ . It is easy to show that, among the first  $\tau$  rounds, by the definition of the disagreement coefficient  $\theta$  and the triangle inequality,

$$\sum_{t=1}^{\tau} \mathbb{E}_{x \sim \mathcal{D}_x} [p_t | \mathcal{F}_{t-1}] \leq \min\{2\theta r_0, 1\} \tau. \quad (17)$$

After  $\tau$  rounds, the label complexity follows directly from Eq. (3) in Theorem 6: by the same argument for the generalization bound (14), with probability at least  $1 - \delta/4$ , we have

$$\begin{aligned} & \sum_{t=\tau+1}^T \mathbb{E}_{x \sim \mathcal{D}_x} [p_t | \mathcal{F}_{t-1}] \\ & \leq \sum_{k=1}^K 4\theta_k \left[ R_k^* T_k' + \sum_{s=T_k-T_k'+1}^{T_k} \sqrt{\frac{8\sigma_T}{s-1}} \right] \\ & \leq \sum_{k=1}^K 4\theta_k \left[ R_k^* T_k' + 2\sqrt{8T_k' \sigma_T} \right], \end{aligned} \quad (18)$$

where the last inequality uses  $\sum_{i=a}^b 1/\sqrt{i} \leq 2(\sqrt{b} - \sqrt{a-1}) \leq 2\sqrt{b-a+1}$ . Combining (17) with (18) concludes the proof.  $\square$

The learning guarantees in Theorem 9 depend on the random quantities  $T_k$  and  $T_k'$ . We can further apply Chernoff's inequality, and relate these random quantities to their expectations.

**Theorem 10** (Chernoff). *Let  $X_1, \dots, X_m$  be independent random variables drawn according to some distribution  $\mathcal{D}$  with mean  $p$  and support included in  $[0, 1]$ . Then, for any  $\gamma \in [0, \frac{1}{p} - 1]$ , the following holds for  $\hat{p} = \frac{1}{m} \sum_{i=1}^m X_i$ :*

$$\begin{aligned} \mathbb{P}[\hat{p} \geq (1 + \gamma)p] & \leq e^{-\frac{m p \gamma^2}{3}}, \\ \mathbb{P}[\hat{p} \leq (1 - \gamma)p] & \leq e^{-\frac{m p \gamma^2}{2}}. \end{aligned}$$

Now we prove Theorem 3.

**Theorem 3.** *Assume that a run of ARBAL over  $T$  rounds has split the input space into  $K$  regions. Then, for any  $\delta > 0$ , with probability at least  $1 - \delta$ , the following inequality holds:*

$$R(\widehat{h}_T) \leq R_U + \sqrt{\frac{32K\sigma_T}{T}} + \frac{16K\sigma_T}{T},$$

where  $R_U = R^* - \gamma(K - 1)$  is an upper bound on the best-in-class error obtained by ARBAL. Moreover, with probability at least  $1 - \delta$ , the expected number of labels requested,  $\tau_T = \sum_{t=1}^T \mathbb{E}_{x_t \sim \mathcal{D}_x} [p_t | \mathcal{F}_{t-1}]$ , satisfies

$$\begin{aligned} \tau_T &\leq \min\{2\theta r_0, 1\}\tau + 4\theta_{\max}(T - \tau) \left[ R_U + 8\sqrt{\frac{K\sigma_T}{T - \tau}} \right] \\ &\quad + \sqrt{32K\sigma_T}. \end{aligned}$$

*Proof.* Given a total of  $T$  samples and a fixed partition, we have  $\mathbb{E}[T_k] = T\mathbf{p}_k$ . By Theorem 10, with probability  $1 - \delta/4$ , for all  $k \in [\kappa]$ ,

$$\frac{T_k}{T} \geq \mathbf{p}_k \left( 1 - \sqrt{\frac{2 \log(\frac{4\kappa}{\delta})}{T\mathbf{p}_k}} \right).$$

By the same covering number argument in Lemma 1, with probability at least  $1 - \delta/4$ , for all partitions and all  $k \in [\kappa]$ ,

$$\frac{T_k}{T} \geq \mathbf{p}_k \left( 1 - \sqrt{\frac{2\kappa D \log(\frac{4\kappa TD}{\delta})}{T\mathbf{p}_k}} \right) \geq \mathbf{p}_k \left( 1 - \sqrt{\frac{2\sigma_T}{T\mathbf{p}_k}} \right).$$

It follows that when  $T \geq \frac{4\sigma_T}{\min_{k \in [\kappa]} \mathbf{p}_k}$  (or equivalently there are at least  $4\sigma_T$  points in each region, which can be easily satisfied), we have

$$\frac{\mathbf{p}_k}{\sqrt{T_k}} \leq \sqrt{\frac{\mathbf{p}_k}{T}} + \frac{2\sqrt{2\sigma_T}}{T}.$$

Plugging into Theorem 9, a union bound implies that with probability at least  $1 - \delta$ ,

$$\begin{aligned} R(\widehat{h}_T) &\leq R^* - \gamma(K - 1) + \sum_{k=1}^K 4\mathbf{p}_k \sqrt{\frac{2\sigma_T}{T_k}} \\ &\leq R^* - \gamma(K - 1) + \sum_{k=1}^K 4\sqrt{\frac{2\mathbf{p}_k\sigma_T}{T}} + \frac{16K\sigma_T}{T}. \end{aligned}$$

Furthermore, by Theorem 10, with probability at least  $1 - \delta/4$ , for all  $k \in [\kappa]$ ,

$$T'_k \leq (T - \tau)\mathbf{p}_k + \sqrt{3(T - \tau)\mathbf{p}_k\sigma_T},$$

which implies that (using the inequality  $\sqrt{x + y} \leq \sqrt{x} + y/(2\sqrt{x})$ )

$$\sqrt{T'_k} \leq \sqrt{(T - \tau)\mathbf{p}_k} + \sqrt{\sigma_T}.$$

Plugging back into Theorem 9, with probability at least  $1 - \delta$ , we have

$$\begin{aligned} &\sum_{t=1}^T \mathbb{E}_{x \sim \mathcal{D}_x} [p_t | \mathcal{F}_{t-1}] \\ &\leq \min\{2\theta r_0, 1\}\tau + \sum_{k=1}^K 4\theta_k \left[ R_k^* T'_k + 4\sqrt{2T'_k\sigma_T} \right] \\ &\leq \min\{2\theta r_0, 1\}\tau + \sum_{k=1}^K 4\theta_k \left[ R_k^* (T - \tau)\mathbf{p}_k \right. \\ &\quad \left. + R_k^* \sqrt{3(T - \tau)\mathbf{p}_k\sigma_T} \right. \\ &\quad \left. + 4\sqrt{2(T - \tau)\mathbf{p}_k\sigma_T} + 4\sqrt{2\sigma_T} \right] \\ &\leq \min\{2\theta r_0, 1\}\tau + \sum_{k=1}^K 4\theta_k \left[ R_k^* (T - \tau)\mathbf{p}_k + \right. \\ &\quad \left. 8\sqrt{(T - \tau)\mathbf{p}_k\sigma_T} \right] + 4K\sqrt{2\sigma_T}, \end{aligned}$$

where the last inequality uses fact that  $R_k^* \leq 1$  and the assumption that  $4\theta_k \leq 1$ , since otherwise the label complexity bound (16) is vacuous.

Using the inequality that  $\sum_{k=1}^K \sqrt{\mathbf{p}_k} \leq \sqrt{K}$ , and  $\sum_{k=1}^K \mathbf{p}_k R_k^* \leq R^* - \gamma(K - 1)$ , we further upper bound the above results. For the generalization error,

$$R(\widehat{h}_T) \leq R^* - \gamma(K - 1) + \sqrt{\frac{32K\sigma_T}{T}} + \frac{16K\sigma_T}{T}.$$

For the expected number of labels,

$$\begin{aligned} &\sum_{t=1}^T \mathbb{E}_{x \sim \mathcal{D}_x} [p_t | \mathcal{F}_{t-1}] \\ &\leq \min\{2\theta r_0, 1\}\tau + \sum_{k=1}^K 4\theta_k \left[ R_k^* (T - \tau)\mathbf{p}_k + \right. \\ &\quad \left. 8\sqrt{(T - \tau)\mathbf{p}_k\sigma_T} \right] + 4K\sqrt{2\sigma_T} \\ &\leq \min\{2\theta r_0, 1\}\tau + 4\theta_{\max} \left[ \left( \sum_{k=1}^K \mathbf{p}_k R_k^* \right) (T - \tau) \right. \\ &\quad \left. + 8 \sum_{k=1}^K \sqrt{(T - \tau)\mathbf{p}_k\sigma_T} \right] + 4K\sqrt{2\sigma_T} \\ &\leq \min\{2\theta r_0, 1\}\tau + 4\theta_{\max}(T - \tau) \left[ R^* - \gamma(K - 1) + \right. \\ &\quad \left. 8\sqrt{\frac{K\sigma_T}{T - \tau}} \right] + \sqrt{32K\sigma_T}. \end{aligned}$$

□

**Determining a fixed  $\gamma$ .** The natural question arises as to how to set the value of threshold  $\gamma$ . Comparing Theorem 3 to the generalization bound of IWAL (Theorem 6), in order for ARBAL to achieve improved guarantees whenever it decides to split ( $K \geq 2$ ), we need to have

$$\begin{aligned} R^* - \gamma(K-1) + \sum_{k=1}^K 2\sqrt{\frac{8\mathfrak{p}_k\sigma_T}{T}} \\ \leq R^* + 2\sqrt{\frac{8\log(2T(T+1)|\mathcal{H}|^2/\delta)}{T}}, \end{aligned}$$

where we have dropped the lower order term  $O(1/T)$ . Neglecting the small differences in the log terms, this turns out to be equivalent to the following condition:

$$2\Delta_T \left[ \sum_{k=1}^K \sqrt{\mathfrak{p}_k} - 1 \right] \leq \gamma(K-1),$$

where  $\Delta_T = \sqrt{8\sigma_T/T}$ . Since  $\sum_{k=1}^K \sqrt{\mathfrak{p}_k} \leq \sqrt{K}$ , and since this analysis applies only when ARBAL decides to split ( $K \geq 2$ ), in order to guarantee improvement over IWAL in the generalization bound for any possible value of  $K$  that ARBAL may select, it is sufficient to impose

$$\begin{aligned} \gamma &\geq 2\Delta_T \left[ \frac{\sqrt{K}-1}{K-1} \right] = \frac{2\Delta_T}{\sqrt{K}+1} \\ \Rightarrow \gamma &\geq \frac{2\Delta_T}{\sqrt{2}+1} = \frac{2}{\sqrt{2}+1} \sqrt{\frac{8\sigma_T}{T}}. \end{aligned}$$

We first prove a more general version of Proposition 4 as follows.

**Lemma 11.** *Let ARBAL run with  $\gamma_t = \mathbb{P}(\mathcal{X}_{k_t})\rho/2$ . With probability at least  $1 - \delta/2$ , for any region  $\mathcal{X}_k$  created during the split phase, it will be split before round  $\left\lceil 2\sigma_T \left(\frac{4}{\rho} + 1\right)^2 / \mathfrak{p}_k \right\rceil$  unless ARBAL has reached the end of the split phase.*

*Proof.* Fix a binary tree and a region  $\mathcal{X}_k$  that is split during the split phase, and assume that splitting  $\mathcal{X}_k$  into  $\mathcal{X}_l \cup \mathcal{X}_r$  satisfies the assumption above. Recall that by assumption, such a split always exists. Then by Lemma 1, with probability at least  $1 - \delta/4$ , the corresponding empirical improvement satisfies

$$\begin{aligned} L_{k,t}(\widehat{h}_{k,t}) - L_{k,t}(\widehat{h}_{l_r,t}) + \Delta(T_{k,t}) \\ \geq R_k(h_k^*) - R_k(h_{l_r}^*) \geq \rho, \end{aligned}$$

where  $\Delta(T_{k,t}) = \sqrt{2\sigma_T/T_{k,t}}$ . Thus, for ARBAL to split

$\mathcal{X}_k$  into  $\mathcal{X}_l, \mathcal{X}_r$ , it is sufficient to have

$$\begin{aligned} L_{k,t}(\widehat{h}_{k,t}) - L_{k,t}(\widehat{h}_{l_r,t}) - \Delta(T_{k,t}) &\geq \rho/2 \\ \Leftrightarrow L_{k,t}(\widehat{h}_{k,t}) - L_{k,t}(\widehat{h}_{l_r,t}) - \Delta(T_{k,t}) \\ &\geq \rho - 2\Delta(T_{k,t}) \geq \rho/2 \\ \Leftrightarrow \Delta(T_{k,t}) &\leq \frac{\rho}{4} \Leftrightarrow T_{k,t} \geq \frac{32\sigma_T}{\rho^2}. \end{aligned}$$

Furthermore, by Theorem 10 and the covering number argument, with probability at least  $1 - \delta/4$ , for all  $t \in [T]$  and all possible partitions with at most  $\kappa$  regions,

$$T_{k,t} \geq t\mathfrak{p}_k \left( 1 - \sqrt{\frac{2\sigma_T}{t\mathfrak{p}_k}} \right),$$

where  $\mathfrak{p}_k = \mathbb{P}(\mathcal{X}_k)$ . Thus, to split  $\mathcal{X}_k$  into  $\mathcal{X}_l \cup \mathcal{X}_r$ , it is sufficient to have

$$T_{k,t} \geq t\mathfrak{p}_k \left( 1 - \sqrt{\frac{2\sigma_T}{t\mathfrak{p}_k}} \right) \geq \frac{32\sigma_T}{\rho^2}.$$

Solving the quadratic inequality and using the fact that  $\sqrt{x+y} \leq \sqrt{x} + \sqrt{y}$  when  $x, y > 0$ , we can write

$$\begin{aligned} t\mathfrak{p}_k \left( 1 - \sqrt{\frac{2\sigma_T}{t\mathfrak{p}_k}} \right) &\geq \frac{32\sigma_T}{\rho^2} \\ \Leftrightarrow \left( \sqrt{t\mathfrak{p}_k} - \sqrt{\sigma_T/2} \right)^2 &\geq \frac{32\sigma_T}{\rho^2} + \frac{\sigma_T}{2} \\ \Leftrightarrow \sqrt{t\mathfrak{p}_k} &\geq \sqrt{\frac{\sigma_T}{2}} + \sqrt{\frac{32\sigma_T}{\rho^2} + \frac{\sigma_T}{2}} \\ \Leftrightarrow \sqrt{t\mathfrak{p}_k} &\geq \sqrt{\frac{\sigma_T}{2}} + \sqrt{\frac{32\sigma_T}{\rho^2}} + \sqrt{\frac{\sigma_T}{2}} \\ \Leftrightarrow t\mathfrak{p}_k &\geq \left( \sqrt{2\sigma_T} + \sqrt{\frac{32\sigma_T}{\rho^2}} \right)^2 \\ \Leftrightarrow t\mathfrak{p}_k &\geq 2\sigma_T \left( \frac{4}{\rho} + 1 \right)^2 \end{aligned}$$

Thus, for ARBAL to split  $\mathcal{X}_k$ , it is sufficient to have

$$t \geq \left\lceil 2\sigma_T \left( \frac{4}{\rho} + 1 \right)^2 / \mathfrak{p}_k \right\rceil.$$

In other words, with probability at least  $1 - \delta/2$ , ARBAL splits region  $\mathcal{X}_k$  before time  $\left\lceil 2\sigma_T \left( \frac{4}{\rho} + 1 \right)^2 / \mathfrak{p}_k \right\rceil$ . The statement holds for all (at most  $\kappa - 1$ ) splits.  $\square$

Thus, Lemma 11 provides an upper bound on the split time for each region created during the split phase. In particular, for the original input space  $\mathcal{X}_k = \mathcal{X}$ ,  $\mathfrak{p}_k = 1$ , and we recover the result of Proposition 4. Combining Lemma 11 with the assumption on the minimal subregion size after each split, we can derive a lower bound on the number of splits ARBAL makes.



**Corollary 5.** Let ARBAL run with  $\gamma_t = \mathbb{P}(\mathcal{X}_{k_t})\rho/2$ . Then, with probability at least  $1 - \delta/2$ , ARBAL splits more than  $\min \left\{ \log_{1/c} \left[ \frac{\tau}{2\sigma_T(4/\rho+1)^2} \right], \kappa - 1 \right\}$  times by the end of the split phase.

*Proof.* Assume that ARBAL has only split  $S < \kappa - 1$  times by the end of  $\tau$  rounds. Then by assumption, the size of any subregion  $\mathcal{X}_k$  satisfies  $\mathbb{P}(\mathcal{X}_k) \geq c^S$ . According to Lemma 11, if

$$\frac{2\sigma_T(4/\rho+1)^2}{p_k} \leq \frac{2\sigma_T(4/\rho+1)^2}{c^S} \leq \tau,$$

then ARBAL must have split the smallest region, thus have more than  $S$  splits. To avoid the contradiction, the number of splits  $S$  must be at least

$$S \geq \log_{1/c} \left[ \frac{\tau}{2\sigma_T(4/\rho+1)^2} \right].$$

Finally, since ARBAL cannot split more than  $\kappa - 1$  times, we have  $S \geq \min \left\{ \log_{1/c} \left[ \frac{\tau}{2\sigma_T(4/\rho+1)^2} \right], \kappa - 1 \right\}$ .  $\square$

Finally, with Corollary 5 handy, we can derive an upper bound on the final best-in-class error after ARBAL's split phase, or equivalently a lower bound on the improvement from a single region's best-in-class error  $R^*$ . We present the full learning guarantees of ARBAL with adaptive  $\gamma_t$  in the following Theorem 12. For simplicity, we assume that the lower bound on  $S$  does not exceed the hard constraint of  $\kappa - 1$ , so that we can get rid of the  $\min\{\cdot\}$  operator.

**Theorem 12.** Assume a run of ARBAL over  $T$  rounds with  $\gamma_t = \mathbb{P}(\mathcal{X}_{k_t})\rho/2$ . Then, with probability at least  $1 - 3\delta/2$ ,

$$\begin{aligned} R(\hat{h}_T) &\leq R_U + 2\sqrt{\frac{8K\sigma_T}{T}} + \frac{16K\sigma_T}{T}, \\ \tau_T &\leq \min\{2\theta r_0, 1\}\tau + 4\theta_{\max}(T - \tau) \left[ R_U + 8\sqrt{\frac{K\sigma_T}{T - \tau}} \right] \\ &\quad + \sqrt{32K\sigma_T}. \end{aligned}$$

where  $R_U = R^* - \frac{\rho c}{2(1-c)} \left(1 - 2\sigma_T \left(\frac{4}{\rho} + 1\right)^2 / \tau\right)$  is an upper bound on the best-in-class error obtained by ARBAL.

*Proof.* When ARBAL splits region  $\mathcal{X}_k$ , by Corollary 2, with high probability, the global best-in-class error is improved by at least  $\mathbb{P}(\mathcal{X}_k) [R_k(h_k^*) - R_k(h_{l_r}^*)] \geq \mathbb{P}(\mathcal{X}_k)\rho/2$ , which means the global improvement depends on the size of the splitting region. Assume ARBAL has made  $S = K - 1$  splits into  $K$  regions. Again, by assumption, at  $s$ -th split,  $s \in [S]$ , the size of the splitting region must be at least  $c^s$ . Thus,

with probability at least  $1 - \delta/2$ , the improvement in the best-in-class error after  $S$  splits is at least

$$\begin{aligned} \frac{\rho}{2} \left( \sum_{s=1}^S c^s \right) &= \frac{\rho c}{2} \left( \frac{1 - c^S}{1 - c} \right) \\ &\geq \frac{\rho c}{2(1-c)} \left( 1 - \frac{2\sigma_T \left(\frac{4}{\rho} + 1\right)^2}{\tau} \right), \end{aligned}$$

where the last inequality follows from the lower bound of  $S$  in Corollary 5. Thus, the best-in-class error after the splits made by ARBAL is upper bounded by

$$R^* - \frac{\rho c}{2(1-c)} \left( 1 - \frac{2\sigma_T \left(\frac{4}{\rho} + 1\right)^2}{\tau} \right),$$

where  $R^*$  is the global best-in-class error on  $\mathcal{X}$  before splitting. The rest of the proof follows from the proof of Theorem 3.  $\square$

Theorem 12 relates the improvement in the best-in-class error with  $c, \rho$  and  $\tau$ . When  $c$  increases, which means ARBAL tends to split more evenly, then there are more improvements in the best-in-class error, partially because there are likely to be more splits. Similarly, when  $\tau$  or  $\rho$  increases, then there tends to be a larger improvement in the best-in-class error, as expected.

Table 1: Binary classification dataset summary:  $N$  denotes the number of samples,  $D$  the number of features (or input space dimension), and  $r$  the relative size of the minority class. Datasets are ordered by increasing  $N$ .

Dataset	$N$	$D$	$r$
kin8nm	8,192	8	0.491
bank8fm	8,192	8	0.404
puma8NH	8,192	8	0.498
visualizing_soil	8,641	4	0.450
delta_elevators	9,517	6	0.497
jm1	10,880	21	0.193
phishing	11,055	68	0.443
mnist35	11,552	784	0.469
egg	14,980	14	0.449
elevators	16,599	18	0.309
magic04	19,020	10	0.352
house16H	22,784	16	0.296
nomao	34,465	118	0.286
fried	40,768	10	0.499
mv	40,768	12	0.403
shuttle	43,500	9	0.216
electricity	45,312	14	0.425
a9a	48,842	123	0.239
ijcnn1	49,990	22	0.097
codrna	59,535	8	0.333
runorwalk	88,588	6	0.499
higgs	98,049	28	0.471
MiniBooNE	130,064	50	0.281
skin	245,057	3	0.208
covtype	581,012	54	0.488

## D. More experimental results

This appendix contains all plots omitted from the main body of the paper.

In Table 1, we show summary statistics for all datasets used in our experiments.

In Figures 4-8, we present the following results for 25 datasets under  $\tau = 800$  and  $\kappa = 20$ : the results of comparing fixed vs. adaptive  $\gamma_t$ , the results of ARBAL as contrasted to the baselines described in the main text, that is, ORIWAL, IWAL, and MARGIN, and the results of ARBAL, using binary tree vs. hierarchical clustering splitting method.

Adaptive  $\gamma_t$  yields superior prediction performance over fixed  $\gamma$  on most datasets, except for `jm1` and `elevators`, where fixed  $\gamma$  rarely splits yet adaptive  $\gamma_t$  fully splits into 20 regions, suggesting that  $\gamma_t$  is overly aggressive due to the simplification of the slack term in the splitting criterion. In the remaining plots, we show the performance of  $\gamma_t$  except for the `jm1` and `elevators` where we use fixed  $\gamma$ .

## Adaptive Region-Based Active Learning

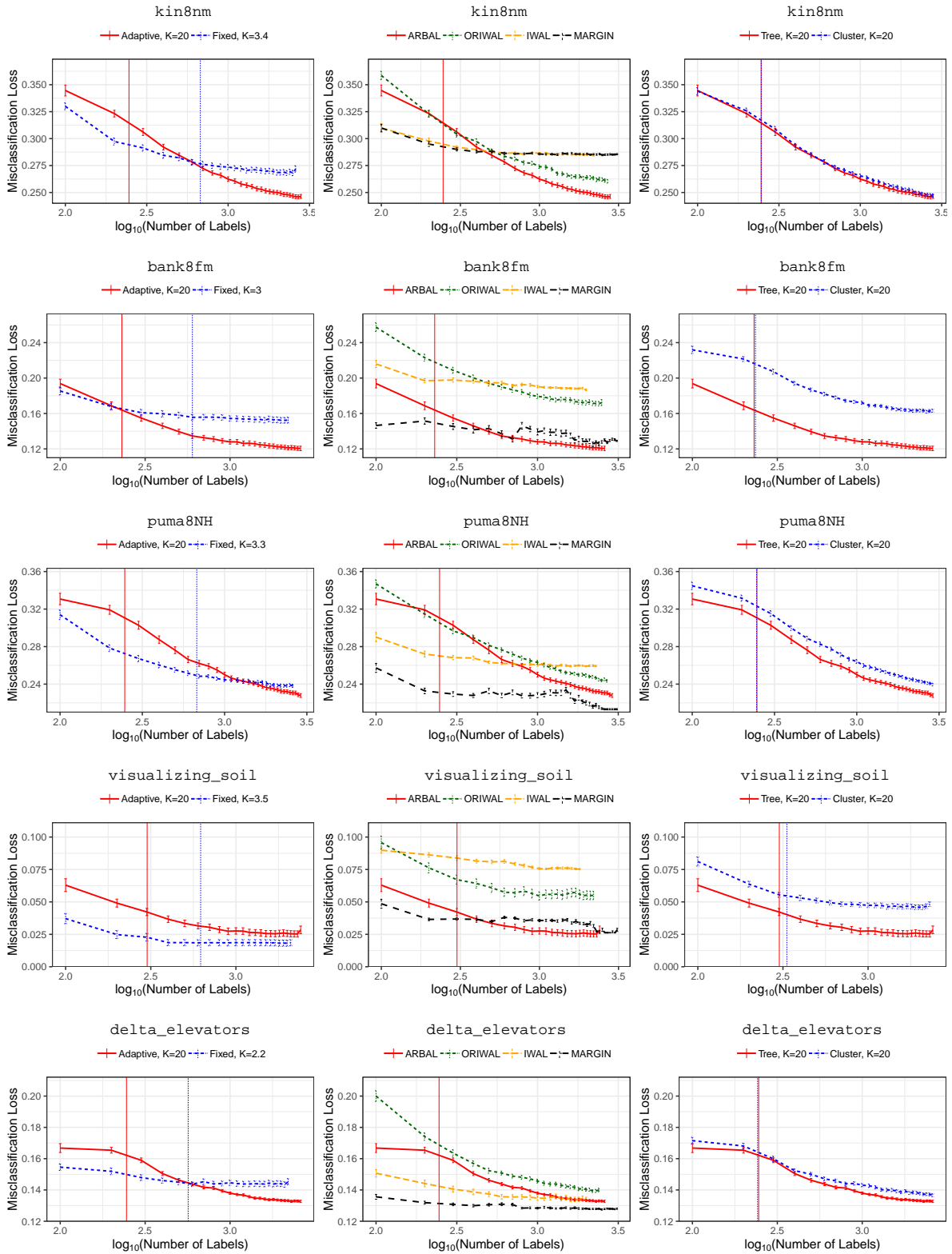


Figure 4: Misclassification loss on hold out test data versus number of labels requested (log<sub>10</sub> scale). Left: ARBAL with fixed and adaptive threshold  $\gamma$ . Middle: ARBAL, RIWAL, IWAL, and MARGIN. Right: ARBAL with different partitioning methods: binary tree and hierarchical clustering. For  $\kappa = 20$  and  $\tau = 800$ , dataset kin8nm, bank8fm, puma8NH, visualizing soil, delta elevators. For left and right plots, we give the average number of resulting regions  $K$  in the legend. The vertical lines indicate when ARBAL transits from the first to the second phase.

## Adaptive Region-Based Active Learning

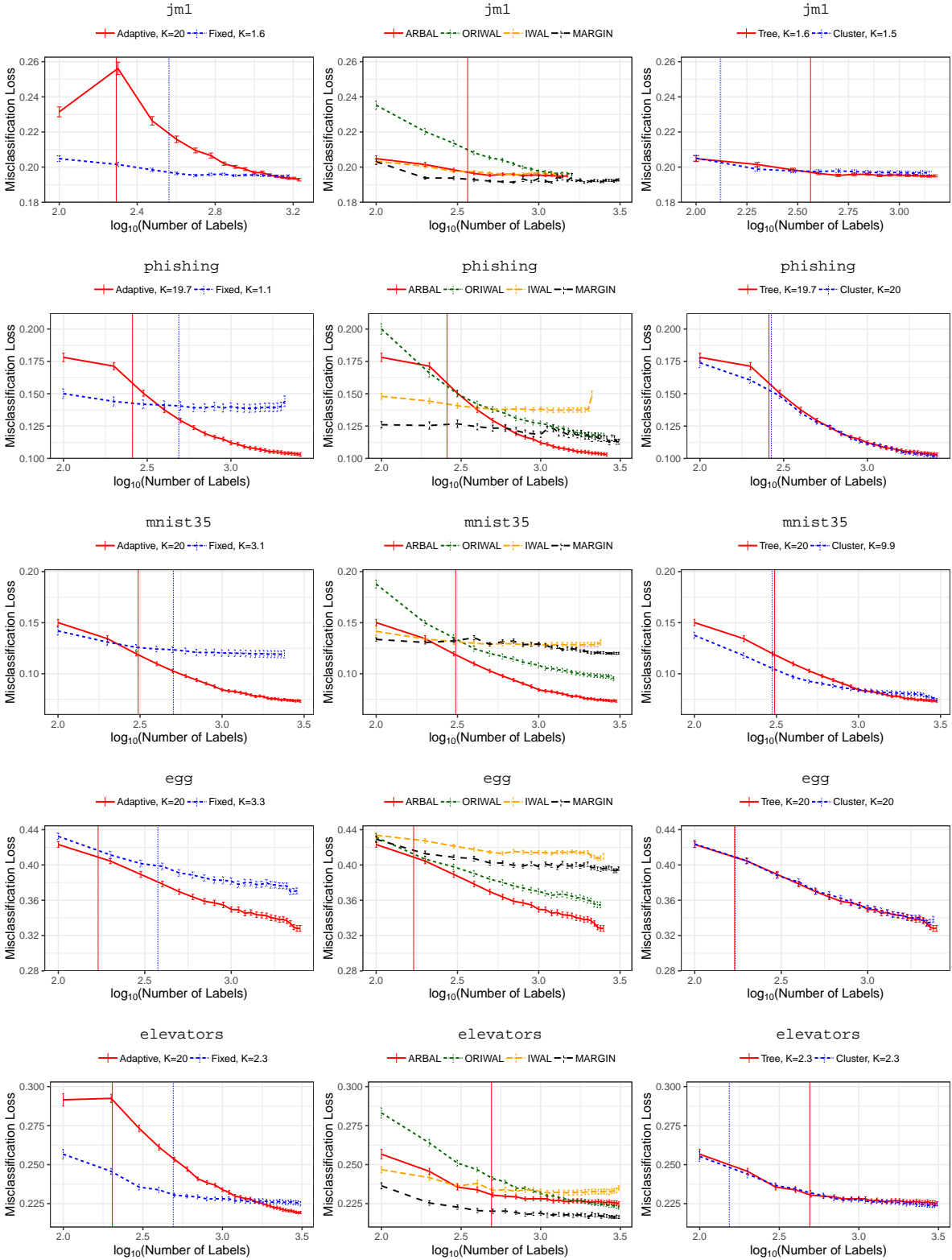


Figure 5: Misclassification loss on hold out test data versus number of labels requested ( $\log_{10}$  scale). Left: ARBAL with fixed and adaptive threshold  $\gamma$ . Middle: ARBAL, RIWAL, IWAL, and MARGIN. Right: ARBAL with different partitioning methods: binary tree and hierarchical clustering. For  $\kappa = 20$  and  $\tau = 800$ , dataset *jml*, *phishing*, *mnist35*, *egg*, *elevators*. For left and right plots, we give the average number of resulting regions  $K$  in the legend. The vertical lines indicate when ARBAL transits from the first to the second phase.

## Adaptive Region-Based Active Learning

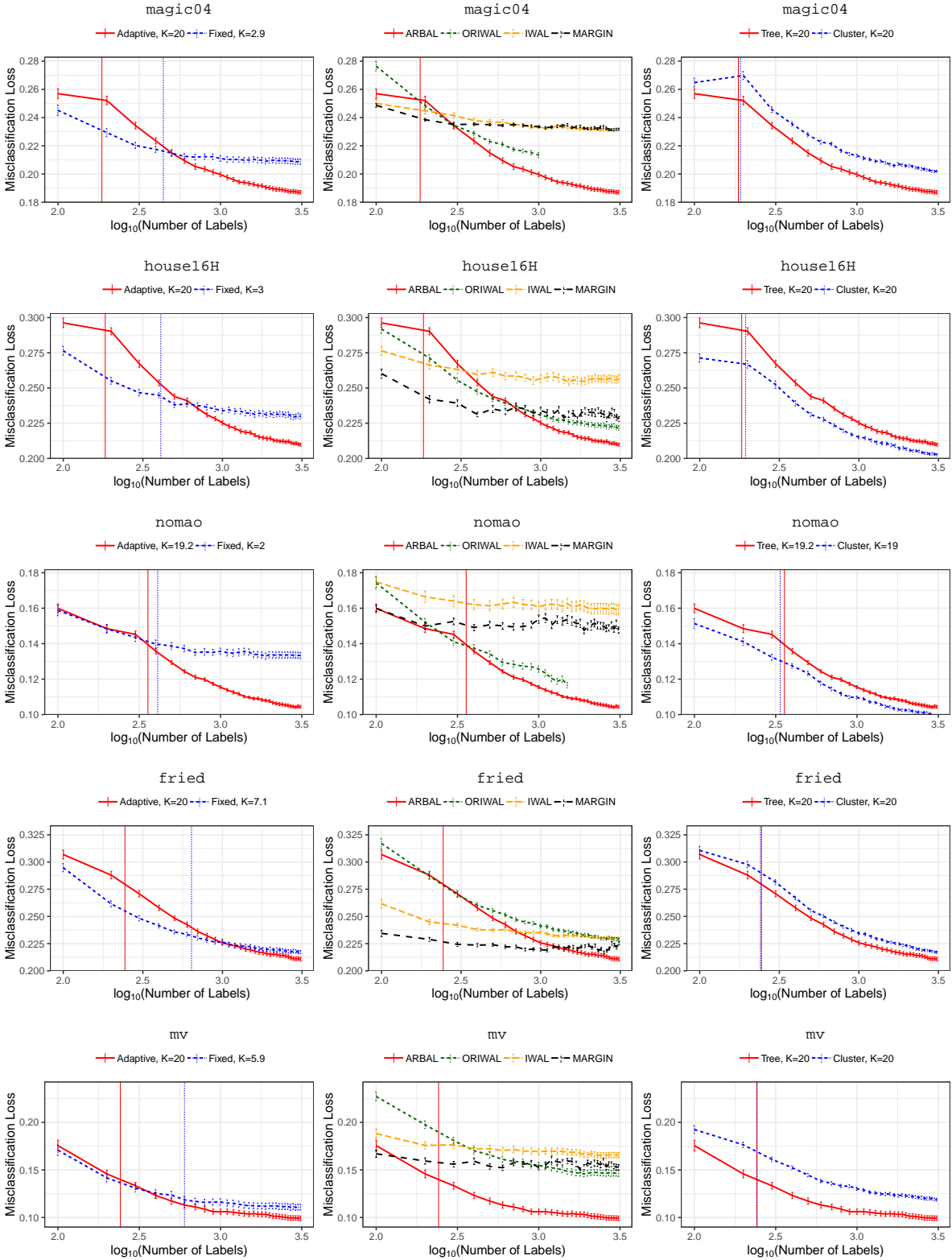


Figure 6: Misclassification loss on hold out test data versus number of labels requested ( $\log_{10}$  scale). Left: ARBAL with fixed and adaptive threshold  $\gamma$ . Middle: ARBAL, RIWAL, IWAL, and MARGIN. Right: ARBAL with different partitioning methods: binary tree and hierarchical clustering. For  $\kappa = 20$  and  $\tau = 800$ , dataset magic04, house16H, nomao, fried, mv. For left and right plots, we give the average number of resulting regions  $K$  in the legend. The vertical lines indicate when ARBAL transits from the first to the second phase.

## Adaptive Region-Based Active Learning

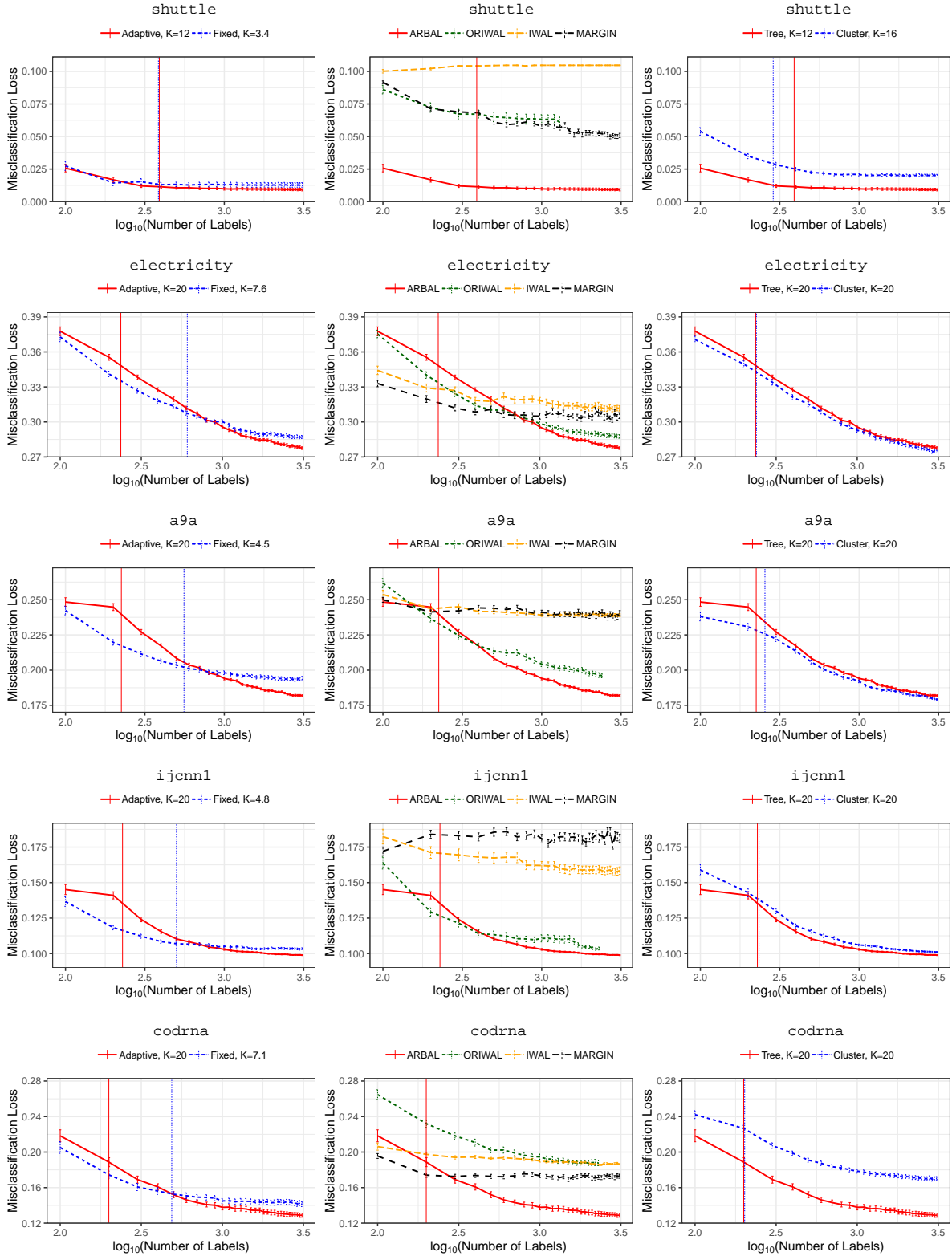


Figure 7: Misclassification loss on hold out test data versus number of labels requested ( $\log_{10}$  scale). Left: ARBAL with fixed and adaptive threshold  $\gamma$ . Middle: ARBAL, RIWAL, IWAL, and MARGIN. Right: ARBAL with different partitioning methods: binary tree and hierarchical clustering. For  $\kappa = 20$  and  $\tau = 800$ , dataset shuttle, electricity, a9a, ijcnn1, codrna. For left and right plots, we give the average number of resulting regions  $K$  in the legend. The vertical lines indicate when ARBAL transits from the first to the second phase.

## Adaptive Region-Based Active Learning

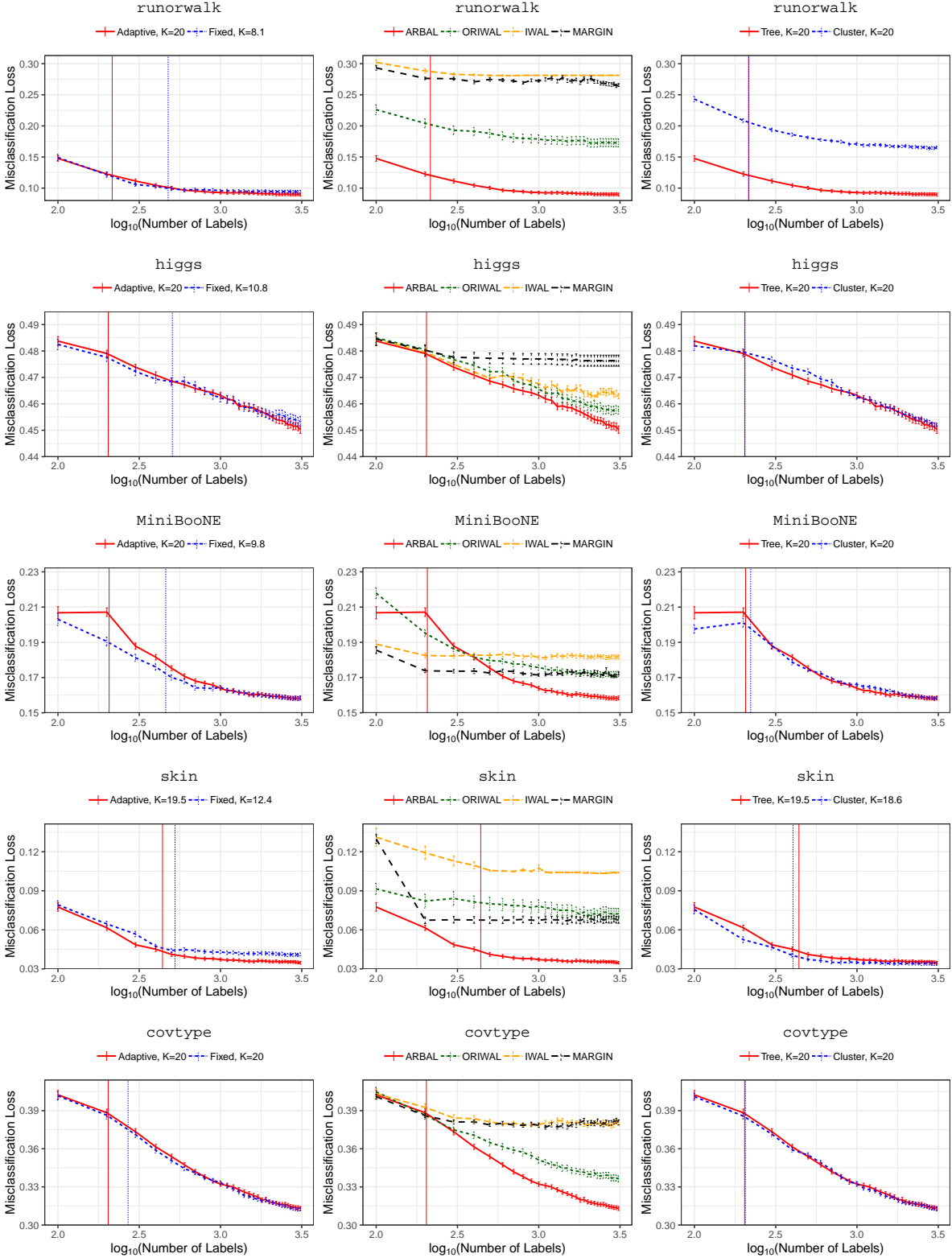


Figure 8: Misclassification loss on hold out test data versus number of labels requested ( $\log_{10}$  scale). Left: ARBAL with fixed and adaptive threshold  $\gamma$ . Middle: ARBAL, RIWAL, IWAL, and MARGIN. Right: ARBAL with different partitioning methods: binary tree and hierarchical clustering. For  $\kappa = 20$  and  $\tau = 800$ , dataset runorwalk, higgs, MiniBooNE, skin, covtype. For left and right plots, we give the average number of resulting regions  $K$  in the legend. The vertical lines indicate when ARBAL transits from the first to the second phase.